



The HTAP_v3.2 emission mosaic: merging regional and global monthly emissions (2000–2020) to support air quality modelling and policies

Diego Guizzardi¹, Monica Crippa¹, Tim Butler², Terry Keating³, Rosa Wu¹⁶, Jacek Kaminski⁴, Jeroen Kuenen⁵, Junichi Kurokawa⁶, Satoru Chatani¹⁵, Tazuko Morikawa⁷, George Pouliot¹⁷, Jacinthe Racine⁸, Michael D. Moran¹⁶, Zbigniew Klimont⁹, Patrick M. Manseau⁸, Rabab Mashayekhi⁸, Barron H. Henderson¹⁷, Steven J. Smith¹⁰, Rachel Hoesly¹⁰, Marilena Muntean¹, Manjola Banja¹¹, Edwin Schaaf¹, Federico Pagani¹¹, Jung-Hun Woo^{13,14}, Jinseok Kim¹⁴, Enrico Pisoni¹, Junhua Zhang¹⁶, David Niemi⁸, Mourad Sassi⁸, Annie Duhamel⁸, Tabish Ansari², Kristen Foley¹⁷, Guannan Geng¹², Yifei Chen¹⁸, and Qiang Zhang¹⁸

¹European Commission, Joint Research Centre (JRC), Ispra, Italy

²Research Institute Sustainability – Helmholtz Centre Potsdam (RIFS Potsdam), Potsdam, 14467, Germany

³U.S. Environmental Protection Agency, Washington DC 20460, USA

⁴Institute of Environmental Protection, National Research Institute, 00-548 Warsaw, Poland

⁵Department of Climate, Air and Sustainability, TNO, Utrecht, the Netherlands

⁶Asia Center for Air Pollution Research (ACAP), 1182 Sowa, Nishi-ku, Niigata-shi 950-2144, Japan

⁷Japan Automobile Research Institute (JARI), Tsukuba, 305-0822, Japan

⁸Air Quality Policy-Issue Response Section, Canadian Centre for Meteorological and Environmental Prediction, Environment and Climate Change Canada (ECCC), Dorval, Quebec, Canada

⁹International Institute for Applied Systems Analysis (IIASA), Laxenburg, Austria

¹⁰Joint Global Change Research Institute, Pacific Northwest National Lab, College Park, MD, USA

¹¹UniSystems Company, Milan, Italy

¹²State Key Joint Laboratory of Environmental Simulation and Pollution Control, School of Environment, Tsinghua University, Beijing 100084, China

¹³Department of Civil and Environmental Engineering, Konkuk University, Seoul, South Korea

¹⁴Department of Technology Fusion Engineering, Konkuk University, Seoul, South Korea

¹⁵National Institute for Environmental Studies (NIES), Tsukuba, 305-8506, Japan

¹⁶Air Quality Research Division, Environment and Climate Change Canada, Toronto, Ontario, Canada

¹⁷U.S. Environmental Protection Agency, 109 T. W. Alexander Drive, Research Triangle Park, North Carolina, USA

¹⁸Ministry of Education Key Laboratory for Earth System Modeling, Department of Earth System Science, Tsinghua University, Beijing 100084, China

Correspondence: Monica Crippa (monica.crippa@ec.europa.eu)

Received: 18 December 2024 – Discussion started: 7 February 2025

Revised: 15 September 2025 – Accepted: 18 September 2025 – Published: 7 November 2025

Abstract. This study, performed under the umbrella of the Task Force on Hemispheric Transport of Air Pollution (TF-HTAP), responds to the need of the global and regional atmospheric modelling community of having a mosaic emission inventory of air pollutants that conforms to specific requirements: global coverage, long time series, spatially distributed emissions with high time resolution, and a high sectoral resolution. The mosaic approach of integrating official regional emission inventories based on locally reported data, with a global inventory based on a globally consistent methodology, allows modellers to perform simulations of a high scientific quality while also ensuring that the results remain relevant to policymakers.

HTAP_v3.2, an ad-hoc global mosaic of anthropogenic inventories, is an update to the HTAP_v3 global mosaic inventory and has been developed by integrating official inventories over specific areas (North America, Europe, Asia including China, Japan and Korea) with the independent Emissions Database for Global Atmospheric Research (EDGAR) inventory for the remaining world regions. The results are spatially and temporally distributed emissions of SO₂, NO_x, CO, NMVOC, NH₃, PM₁₀, PM_{2.5}, Black Carbon (BC), and Organic Carbon (OC), with a spatial resolution of 0.1 × 0.1° and time intervals of months and years covering the period 2000–2020 (<https://doi.org/10.5281/zenodo.17086684>, Crippa, 2025, https://edgar.jrc.ec.europa.eu/dataset_htap_v32, last access: 27 October 2025). The emissions are further disaggregated to 16 anthropogenic emitting sectors. This paper describes the methodology applied to develop such an emission mosaic, reports on source allocation, differences among existing inventories, and best practices for the mosaic compilation. One of the key strengths of the HTAP_v3.2 emission mosaic is its temporal coverage, enabling the analysis of emission trends over the past two decades. The development of a global emission mosaic over such long time series represents a unique product for global air quality modelling and for better-informed policy making, reflecting the community effort expended by the TF-HTAP to disentangle the complexity of transboundary transport of air pollution.

1 Introduction

Common international efforts have procured an agreement to reduce global air pollutant emissions. For this purpose, the United Nations Economic Commission for Europe (UNECE) Convention on Long Range Transboundary Air Pollution (CLRTAP) and the Task Force on Hemispheric Transport of Air Pollution (TF-HTAP) have been instrumental in developing the understanding of intercontinental transport of air pollution and thus contributing to the reduction of key pollutants in Europe and North America.

The success of CLRTAP is based on meeting strict reduction targets for pollutant releases. Therefore, evaluating the resulting implications of these reductions requires an ongoing improvement of global emission inventories in terms of emission updating and of methodological refinements. These aspects are instrumental to gain understanding of transboundary air pollution processes and drivers and to measure the effectiveness of emissions reduction and air quality mitigation policies. New guidance is available to achieve further emission reductions across all emitting sectors. An example is the establishment of the Task Force for International Cooperation on Air Pollution in 2019, which is intended to promote international collaboration for preventing and reducing air pollution and improving air quality globally (UNECE, 2021). As part of the ongoing effort by CLRTAP to reduce emissions and to set out more effective and accountable mitigation measures, the 2005 Gothenburg Protocol (UNECE, 2012) has been revised, including the review of the obligations in relation to emission reductions and mitigation measures (e.g., black carbon and ammonia) and the review of the progress towards achieving the environmental and health objectives of the Protocol.

The Task Force on Hemispheric Transport of Air Pollution (TF-HTAP) of the Convention has a mandate to promote the scientific understanding of the intercontinental transport of air pollution to and from the UNECE area (<https://unece.org/>

geographical-scope, last access: 27 October 2025), to quantify its impacts on human health, vegetation and climate, and to identify emission mitigation options that will shape future global policies.

This paper describes and discusses a consistent global emission inventory of air pollutants emitted by anthropogenic activities. This important database has been developed to assess the contribution of anthropogenic air pollution emission sources within and outside the UNECE-area through atmospheric modelling. This inventory has been compiled based on officially reported emissions, and an independent global inventory where officially reported emissions are not used. This harmonised emissions “mosaic” dataset, hereafter referred to as the HTAP_v3.2, contains annual and monthly:

- emission time series (from 2000 to 2020) of SO₂, NO_x (expressed as NO₂ mass unit), CO, NMVOC, NH₃, PM₁₀, PM_{2.5}, BC, OC by emitting sector and country, and
- spatially distributed emissions on a global grid with spatial spacing of 0.1 × 0.1°.

1.1 Brief description of the previous version of this dataset (HTAP_v3)

The creation of a global emission mosaic requires the harmonisation of several data sources, detailed analysis of contributing sectors for the different input inventories, development of data quality control procedures, and a robust and consistent gap-filling methodology when lacking information. The development of the HTAP_v3 global mosaic inventory (Crippa et al., 2023) built upon the previous experience of the HTAPv1 (Janssens-Maenhout et al., 2012) and HTAPv2.2 (Janssens-Maenhout et al., 2015) global inventories. HTAP_v3, as requested by the TF-HTAP modelling community, provided a more refined sectoral disaggregation

compared to the previous HTAP emission mosaics. It also included tools (https://edgar.jrc.ec.europa.eu/htap_tool/, last access: 27 October 2025) that allow the extraction of emission data over selected domains (detailed later in Sect. 4).

The HTAP_v3 mosaic was composed by integrating official, spatially distributed emissions data from the Copernicus Atmosphere Monitoring Service Regional inventory CAMS-REG-v5.1 (Kuenen et al., 2022), US EPA (U.S. Environmental Protection Agency, 2021b, a; Foley et al., 2023), Environment and Climate Change Canada (ECCC) (NPRI, 2017), the Regional Emission inventory in ASia (REAS), CAPSS-KU, and JAPAN (<https://www.env.go.jp/air/osen/pm/inventory.html>, last access: 27 October 2025) (Kurokawa and Ohara, 2020; Chatani et al., 2018, 2020) inventories. As the information gathered from the official reporting covers only part of the globe, HTAP_v3 was completed using emissions from the Emissions Database for Global Atmospheric Research (EDGAR) version 6.1 (https://edgar.jrc.ec.europa.eu/dataset_ap61, last access: 27 October 2025).

One of the key strengths of the HTAP_v3 emission mosaic was the temporal coverage of the emissions, spanning the 2000–2018 period, enabling the analysis of emission trends over the past two decades. The development of a global emission mosaic over such long time series represented a unique product for air quality modelling and for better-informed policy making, reflecting the effort of the TF-HTAP community to improve understanding of the transboundary transport of air pollution. The year 2000 was chosen as the start year since it often represents the year from which complete datasets of annual air pollutant emissions can be generated. It also represents a turning point for several emerging economies (e.g., China) and the strengthening of mitigation measures in historically developed regions (e.g., EU, USA, etc.).

The two previous generations of HTAP emission mosaics had limited temporal coverage. HTAPv1 covered the period 2000–2005 with annual resolution (https://edgar.jrc.ec.europa.eu/dataset_htap_v1, last access: 27 October 2025, Janssens-Maenhout et al., 2012), while HTAPv2.2 covered two recent years (2008 and 2010), but with monthly resolution (Janssens-Maenhout et al., 2015) (https://edgar.jrc.ec.europa.eu/dataset_htap_v2, last access: 27 October 2025). However, the needs of the TF-HTAP modelling community are continuously evolving to both foster forward-looking air quality science and produce more fit-for-purpose analyses in support of efficient policy making. HTAP_v3 therefore not only covers the time period of the previous HTAP phases, but also extends it forward by almost a decade, to provide the most up-to-date picture of global air pollutant emission trends. Another distinguishing feature of the HTAPv3 mosaic is a considerably higher sectoral resolution than previous iterations of the HTAP mosaic inventories (Sect. 2.2), enabling more policy-relevant use of the inventory.

1.2 Use and impact of the HTAP_v3 global mosaic emission dataset

At the time of publishing this work (October 2025), the dataset description paper for the HTAPv3 global mosaic emission inventory (Crippa et al., 2023) has been cited 80 times in Scopus, achieving a field-weighted citation index of 4.10, putting it in the 96th percentile for the number of citations compared with similar publications.

Of the studies in which the use of HTAPv3 emission dataset has played a significant role, the primary use of the dataset has been as input data for modelling studies, almost all with a regional focus (Chutia et al., 2024; Clayton et al., 2024; Graham et al., 2024; Hu et al., 2024; Itahashi, 2023; Itahashi et al., 2024; Kim et al., 2024, 2023b; Liu et al., 2024; Nawaz et al., 2023; Sharma et al., 2023, 2024; Thongsame et al., 2024; Wang et al., 2024). While the upcoming HTAP3-Fires multi-model study (Whaley et al., 2025), with a global focus on the influence of wildfire emissions on air quality, plans to use the HTAPv3.2 dataset for anthropogenic emissions, so far only one study has appeared in the literature using the HTAPv3 dataset as input for a modelling study with a primarily global focus (Nalam et al., 2025). The mosaic approach used in the development of the HTAPv3 emission data makes it especially interesting for regional modelers, as the spatial distribution of emissions in the component regional inventories is preserved in the final dataset. Furthermore, the use of gap-filling for missing sectors or regions outside of the domain of the component regional inventories, but within the domain of the regional model, allows regional modelers to avoid the need to perform their own gap-filling when preparing their emission data.

Another use of the dataset has been as a benchmark for the evaluation of other emission inventories, including other bottom-up inventories (Huang et al., 2023; Soulie et al., 2024; Xu et al., 2024), as well as emission estimates based on assimilation of satellite observations (Ding et al., 2024; Mao et al., 2024; van Der A et al., 2024; Zhao et al., 2024) and inverse modelling of surface observations (Kong et al., 2024). Several other studies have used emissions information from the HTAPv3 dataset as a reference in their interpretation of air quality observations and their trends (Kim et al., 2023a; Patel et al., 2024; Smaran and Vinoj, 2024).

1.3 Update to HTAP_v3.2

As modelers often require up-to-date emission data for the simulation of recent historical periods, emission datasets must be continuously updated. For officially reported emission data, these updates however often lag several years behind the current year. The Task Force on Hemispheric Transport is currently planning a set of multi-model experiments of the recent historical period. In order to be as relevant as possible, this study should include as many recent years as possible. Since the release of the original HTAP_v3 dataset

in April 2023, several of the regional data providers have updated their emission inventories. The global base inventory has also been updated to EDGAR version 8. With the update from HTAP_v3 to HTAP_v3.2, it is now possible to extend the timeseries of the global mosaic emissions until the year 2020.

Furthermore, in the original HTAP_v3 dataset, emissions from China were included from the pan-regional REAS inventory, rather than the Multi-resolution Emission Inventory for China (MEIC). The update from HTAP_v3 to HTAP_v3.2 also provides the opportunity to include the MEIC emissions for China, allowing the use of the best available regional emissions for model simulations of air quality in China and in regions influenced by emissions from China.

The update from HTAP_v3 to HTAP_v3.2 also provides the opportunity to respond to feedback from users of the original HTAP_v3 data, including the improvement of the regional datasets. These updates are described below. Major changes within each data source compared to HTAP_v3 are summarized in Table 5.

The methodology and data sources for the HTAP_v3.2 emission mosaic are described in Sect. 2. The long-time coverage of two decades, allows comprehensive trend analysis (see Sect. 3), the HTAP_v3 data format and data-set access are presented in Sect. 4 and conclusions are provided in Sect. 5.

2 HTAP_v3.2 emission mosaic overview: data sources, coverage, and methodology

2.1 Data input

The HTAP_v3.2 mosaic is a database of monthly- and sector-specific global air pollutant emission gridmaps developed by integrating spatially explicit regional information from recent officially reported national or regional emission inventories. Data from seven main regional inventories were integrated into HTAP_v3.2, which covered only North America, Europe, and a portion of Asia (including Japan, China, India, and South Korea) (Fig. 1). The geographical domain covered by each of these inventories is depicted in Fig. 1, while further details on each contributing inventory are presented in Sect. 2.3. The emissions for all other countries, international shipping and aviation (international and domestic) have been retrieved from the Emissions Database for Global Atmospheric Research (EDGARv8.1, https://edgar.jrc.ec.europa.eu/dataset_ap81, last access: 27 October 2025) as represented by the grey areas in Fig. 1. Depending on the pollutant, more than half of global emissions are provided by region-specific inventories, while the remaining contribution is derived from the EDGAR global inventory as reported in the bar graph of Fig. 1, where the share of each individual inventory to global emissions is represented. For all pollutants, the Asian domain is contributing most to global emissions,

hence the importance of having accurate emission inventories for this region.

Recent literature studies (Puliafito et al., 2021; Huneus et al., 2020; Álamos et al., 2022; Keita et al., 2021) document additional regional/local inventories which may contribute to future updates of HTAP_v3.2, in particular extending the mosaic compilation to regions in the Southern Hemisphere. Considering relative hemispheric emission levels as well as the atmospheric dynamics happening in the Northern Hemisphere and regulating the transboundary transport of air pollution, the current HTAP_v3.2 mosaic should still satisfy the needs of the atmospheric modelling community, although improvements using latest available inventories for Africa and South America may also be considered for future updates.

Table 1 provides an overview of all data providers, in terms of geographical and temporal coverage, data format, and sectoral and pollutant data availability. Table 2 defines the HTAP_v3.2 sectors and corresponding Intergovernmental Panel on Climate Change (IPCC) codes. Table 3 further details the sector-pollutant data availability for each inventory and the gap-filling approach required for some sectors and pollutants.

2.2 Pollutant, spatial, temporal and sectoral coverage

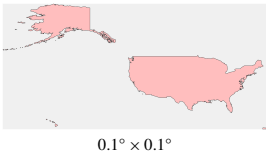
The HTAP_v3.2 emission mosaic helps to address the transboundary role of air pollutants by providing a key input for atmospheric modellers and supporting the evaluation of environmental impact analyses for poor air quality. For this reason, HTAP_v3.2 provides global $0.1 \times 0.1^\circ$ emission gridmaps for all air pollutants and specifically for acidifying and eutrophying gases (such as SO_2 , NH_3 , NO_x), ozone precursors (NMVOC, CO, NO_x), and primary particulate matter (PM_{10} , $\text{PM}_{2.5}$, BC, OC).

Emissions from each officially reported inventory were submitted to HTAP on $0.1 \times 0.1^\circ$ regional gridmaps. Spatial allocation was performed to these gridmaps for each sector by each inventory group using the best available set of subsector spatial surrogate fields used by each group. EDGARv8.1 global gridmaps are also on a $0.1 \times 0.1^\circ$ grid.

Compared to the two previous HTAP emission mosaics, HTAP_v3.2 input emission gridmaps were provided with monthly time distributions to better reflect the regional seasonality of sector specific emissions (e.g., household, power generation, and agricultural activities). Information on emission peaks over certain months of the year is also a useful information for the development of territorial policies to mitigate localised emission sources in space and time (e.g., emissions from residential heating over winter months, agricultural residue burning, etc.).

The HTAP_v3.2 mosaic provides emissions for gaseous and particulate matter air pollutants arising from all anthropogenic emitting sectors except for wildfires and savannah burning, which represent major sources of particulate mat-

Table 1. Overview of data input to the HTAP_v3.2 emission mosaic. For each data source all substances (SO₂, NO_x, CO, NMVOC, NH₃, PM₁₀, PM_{2.5}, BC, OC) are provided.

Data source	Sectors	Time coverage and resolution	Geocoverage and spatial resolution	References
CAMS-REG-v6.1	All*	2000–2020 Annual emission gridmaps + monthly profiles	 0.1° × 0.1°	Kuenen et al. (2022)
US EPA	All*	2002–2020 Monthly emission gridmaps	 0.1° × 0.1°	U.S. Environmental Protection Agency (2021a, b), Foley et al. (2023)
ECCC	All*, excluding agricultural waste burning	2000–2019 Monthly emission gridmaps	 0.1° × 0.1°	APEI (2018, 2021)
REASv3.2.1	All*, excluding brake and tyre wear, domestic shipping, waste, agricultural waste burning	2000–2015 Monthly emission gridmaps	 0.1° × 0.1° (The original spatial resolution of REASv3.2.1 is 0.25° × 0.25°. Assuming that emissions are equally distributed in the 0.25° cell, REASv3.2.1 data were converted to 0.1° cell and provided to HTAP_v3.2)	https://www.nies.go.jp/REAS/ (last access: June 2023), Kurokawa and Ohara (2020)
CAPSS-KU	All* gridmaps + monthly profiles	2000–2018 Annual emission	 0.1° × 0.1°	
JAPAN (PM _{2.5} EI and J-STREAM)	All*	2000–2020 Monthly emission gridmaps	 0.1° × 0.1°	https://www.env.go.jp/air/osen/pm/inventory.html (last access: December 2024); Shibata and Morikawa, (2021); Chatani et al. (2020)
MEICv1.4	All*, excluding brake and tyre wear, waste and agricultural waste burning	2000–2020 Monthly emission gridmaps	 0.1° × 0.1°	http://meicmodel.org.cn/ (last access: December 2024); Geng et al. (2024)
EDGARv8.1	All*	2000–2020 Monthly emission gridmaps	 0.1° × 0.1°	https://edgar.jrc.ec.europa.eu/dataset_ap81 (last access: December 2024)

* International shipping and aviation (international and domestic) are fully provided by EDGAR.

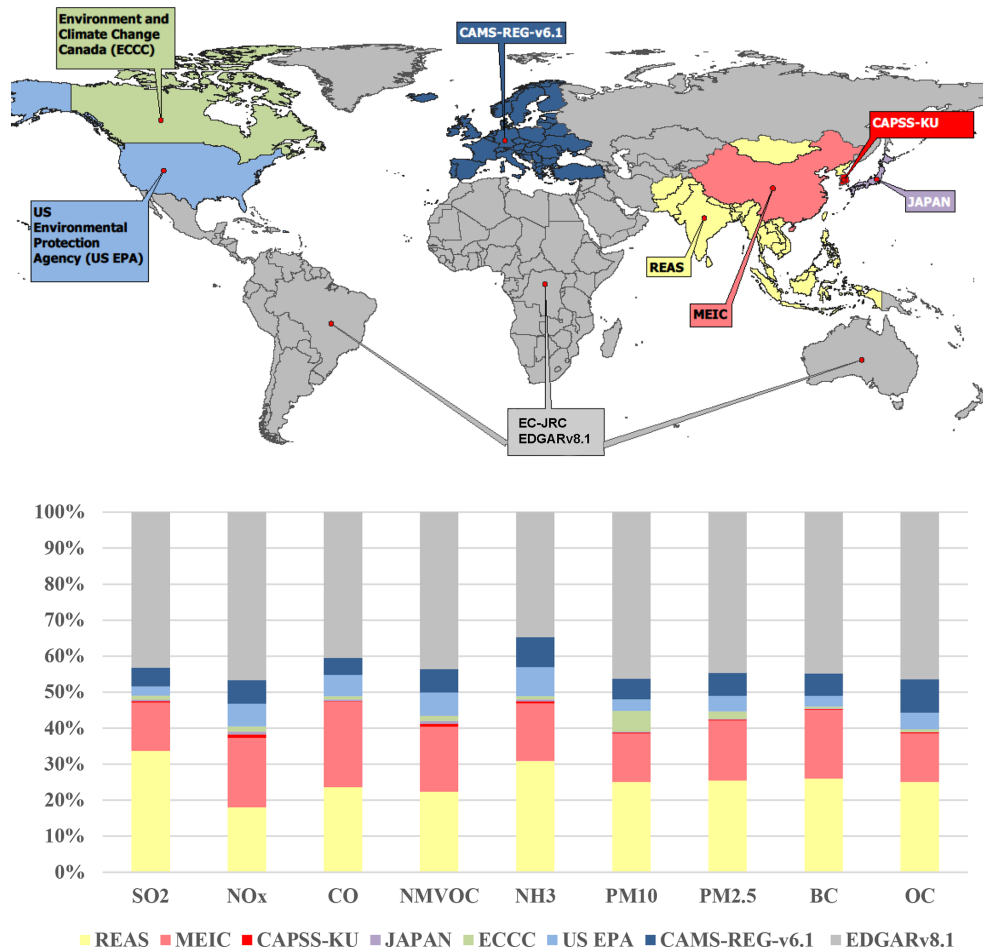


Figure 1. Overview of the HTAP_v3.2 mosaic data providers. Data from officially reported emission grid maps were collected from the US Environmental Protection Agency, Environment and Climate Change Canada, CAMS-REG-v6.1 for Europe, REASv3.2.1 for most of the Asian domain, CAPSS-KU for South Korea, MEICv1.4 for China and JAPAN (PM_{2.5}EI and J-STREAM) for Japan. EDGARv8.1 is used as gap-filling inventory. The share of the total emissions covered by each data provider is reported in the bar chart at the bottom.

ter and CO emissions. Wildfires and savannah burning are not included in the current mosaic since community efforts are ongoing to tackle these sources specifically. Modellers can find these additional sources on several publicly available global wildfire emission datasets compiled based on the best available scientific knowledge, such as the Global Fire Emission Database (GFED, <https://www.globalfiredata.org/>, last access: 27 October 2025) or the Global Wildfire Information System (GWIS, <https://gwis.jrc.ec.europa.eu/>, last access: 27 October 2025). When using satellite retrieved emissions from fires, they should be treated with caution to avoid double counting the emissions released by e.g. agricultural crop residue burning activities.

HTAP_v3.2 provides emissions at higher sectoral disaggregation than previous HTAP experiments¹ to better

¹HTAPv1 covered 10 broad emission sectors (Aircraft, Ships, Energy, Industry Processes, Ground Transport, Residential, Solvents, Agriculture, Agriculture Waste Burning, and Waste), while

understand drivers of emission trends and the effectiveness of sector-specific policy implementation. Emissions from 16 sectors are provided by the HTAP_v3.2 mosaic, namely: International Shipping; Domestic Shipping; Domestic Aviation; International Aviation; Energy; Industry; Fugitives; Solvent Use; Road Transport; Brake and Tyre Wear; Other Ground Transport; Residential; Waste; Agricultural Waste Burning; Livestock; and Agricultural Crops. Further details on the sector definitions as well as their correspondence with the IPCC codes (IPCC, 1996, 2006) are provided in Table 2. The selection of the number of sectors was constrained by the sectoral disaggregation of the input inventories (see Table S1 in the Supplement). Table 3 provides the complete overview of the emission data provided by each inventory group indicating the pollutants covered for each sector and eventual

even broader sectoral emissions were provided in HTAPv2.2 (Air, Ships, Energy, Industry, Transport, Residential (including waste), and Agriculture (only for NH₃)).

Table 2. Definition of HTAP_v3.2 sectors and correspondence to IPCC codes.

HTAP_v3 main sectors	HTAP_v3.2 detailed sectors	Sector description	IPCC 1996 codes	IPCC 2006 codes
HTAP_1: International Shipping	HTAP_1: International Shipping	International water-borne navigation.	1C2	1.A.3.d.i
HTAP_2: Aviation	HTAP_2.1.1: Domestic Aviation LTO	Domestic Aviation landing&takeoff.	1A3aii	1.A.3.a.ii
	HTAP_2.1.2: Domestic Aviation CDS	Domestic Aviation climbing&descent.	1A3aii	1.A.3.a.ii
	HTAP_2.1.3: Domestic Aviation CRS	Domestic Aviation cruise.	1A3aii	1.A.3.a.ii
	HTAP_2.2.1: International Aviation LTO	International Aviation landing&takeoff.	1A3ai	1.A.3.a.i
	HTAP_2.2.2: International Aviation CDS	International Aviation climbing&descent.	1A3ai	1.A.3.a.i
	HTAP_2.2.3: International Aviation CRS	International Aviation cruise.	1A3ai	1.A.3.a.i
HTAP_3: Energy	HTAP_3: Energy	Power generation.	1A1a	1.A.1.a
HTAP_4: Industry	HTAP_4.1: Industry	Industrial non-power large-scale combustion emissions and emissions of industrial processes. It includes: manufacturing, mining, metal, cement, chemical and fossil fuel fires.	1A2 + 2 + 5B	1A2 + 2 (excluding 2.D.3 + 2.E + 2.F + 2.G) + 7A
	HTAP_4.2: Fugitive	It includes oil and gas exploration and production and transmission, including evaporative emissions (mainly NMVOC).	1B + 1A1b + 1A1ci + 1A1cii + 1A5biii	1.B + 1.A.1.b + 1.A.1.c.i + 1.A.1.c.i.i + 1.A.5.b.i.i.i
	HTAP_4.3: Solvents	Solvents and product use.	3	2D3 + 2E + 2F + 2G
HTAP_5: Ground Transport	HTAP_5.1: Road Transport	Road Transport, combustion and evaporative emissions only.	1A3b (excluding resuspension)	1.A.3.b (excluding resuspension)
	HTAP_5.2: Brake and Tyre wear	Re-suspended dust from pavements or tyre and brake wear from road transport.	1A3b (resuspension only)	1.A.3.b (resuspension only)
	HTAP_5.3: Domestic shipping	Domestic shipping: inland waterways + domestic shipping.	1A3d2	1.A.3.d.ii
	HTAP_5.4: Other ground transport	Ground transport by pipelines and other ground transport of mobile machinery.	1A3c + 1A3e	1.A.3.c + 1.A.3.e.ii
HTAP_6: Residential	HTAP_6: Residential	Small-scale combustion, including heating, cooling, lighting, cooking and auxiliary engines, to equip residential, commercial buildings, service institutes, and agricultural facilities and fisheries.	1A4 + 1A5	1.A.4 + 1.A.5
HTAP_7: Waste	HTAP_7: Waste	Solid waste disposal and wastewater treatment.	6	4
HTAP_8: Agriculture	HTAP_8.1: Agricultural waste burning	Agricultural waste burning (excluding Savannah burning).	4F	3.C.1.b
	HTAP_8.2: Agriculture livestock	Livestock emissions, including manure management.	4B	3.A.2
	HTAP_8.3: Agriculture crops	Emissions from crops, fertilisers, and all agricultural soils activities.	4C + 4D	3.C.2 + 3.C.3 + 3.C.4 + 3.C.7

Table 3. Overview of pollutant and sector provided by each inventory in HTAP_v3.2. “ALL” indicates that all substances are provided. “N/A” indicates that the emissions for those sectors were not provided and/or used in HTAP_v3.2 for a specific inventory and were gap-filled with the corresponding information from EDGARv8.1. The other cells represent the data availability for each sector and inventory. The pollutants’ font style refers to the data source: plain text represents pollutant emissions provided by a specific inventory, bold indicates emissions gap-filled using EDGARv8.1, and italic indicates combinations of sectors–pollutants available for specific regional inventories but not in EDGAR, which typically represents minor sources of emissions included in officially reported inventories. These minor sources are included in the HTAP_v3.2 mosaic.

Data provider	REAS v3.2.1	CAPSS-KU	MEICv1.4	JAPAN	ECCC	US EPA	CAMS-REG-v6.1	EDGARv8.1
HTAP_1: International Shipping	N/A	N/A	N/A	N/A	N/A	N/A	N/A	ALL
HTAP_2.1: Domestic Aviation	N/A	N/A	N/A	N/A	N/A	N/A	N/A	ALL
HTAP_2.2: International Aviation	N/A	N/A	N/A	N/A	N/A	N/A	N/A	ALL
HTAP_3: Energy	ALL	ALL	BC, OC, NO _x , NH ₃ , CO, PM _{2.5} , PM ₁₀ , NMVOC, SO ₂	BC, OC, NO _x , NH ₃ , CO, PM _{2.5} , PM ₁₀ , NMVOC, SO ₂	ALL	ALL	ALL	ALL
HTAP_4.1: Industry	ALL	ALL	ALL	BC, OC, NO _x , NH ₃ , CO, PM _{2.5} , PM ₁₀ , NMVOC, SO ₂	ALL	ALL	ALL	ALL
HTAP_4.2: Fugitive	ALL	BC, OC, NO _x , NH ₃ , CO, PM _{2.5} , PM ₁₀ , NMVOC, SO ₂	BC, OC, NO _x , NH ₃ , CO, PM _{2.5} , PM ₁₀ , NMVOC, SO ₂	BC, OC, NO _x , NH ₃ , CO, PM _{2.5} , PM ₁₀ , NMVOC, SO ₂	ALL	ALL	ALL	ALL
HTAP_4.3: Solvents	NMVOC, NH ₃ , PM ₁₀ , PM _{2.5}	NMVOC, NH ₃ , PM ₁₀ , PM _{2.5}	NMVOC, NH ₃ , PM ₁₀ , PM _{2.5}	NMVOC, NH ₃ , PM ₁₀ , PM _{2.5}	NMVOC, NH ₃ , PM ₁₀ , PM _{2.5}	CO, NO _x , OC, NMVOC, NH ₃ , PM ₁₀ , PM _{2.5} , SO ₂	NO _x , NH ₃ , CO, PM _{2.5} , PM ₁₀ , NMVOC, SO ₂	NMVOC, NH ₃ , PM ₁₀ , PM _{2.5}
HTAP_5.1: Road Transport	ALL	ALL	ALL	ALL	ALL	ALL	ALL	ALL
HTAP_5.2: Brake and Tyre wear	N/A	BC, OC, PM _{2.5} , PM ₁₀	BC, OC, PM _{2.5} , PM ₁₀	BC, OC, PM _{2.5} , PM ₁₀	BC, OC, PM _{2.5} , PM ₁₀	BC, OC, PM _{2.5} , PM ₁₀	BC, OC, PM _{2.5} , PM ₁₀	BC, OC, PM _{2.5} , PM ₁₀
HTAP_5.3: Domestic shipping	N/A	ALL	BC, OC, NO _x , NH ₃ , CO, PM _{2.5} , PM ₁₀ , NMVOC, SO ₂	N/A	ALL	ALL	BC, OC, NO _x , NH ₃ , CO, PM _{2.5} , PM ₁₀ , NMVOC, SO ₂	ALL
HTAP_5.4: Other ground transport	ALL	ALL	BC, OC, NO _x , NH ₃ , CO, PM _{2.5} , PM ₁₀ , NMVOC, SO ₂	BC, OC, NO _x , NH ₃ , CO, PM _{2.5} , PM ₁₀ , NMVOC, SO ₂	ALL	ALL	ALL	ALL
HTAP_6: Residential	ALL	ALL	ALL	BC, OC, NO _x , NH ₃ , CO, PM _{2.5} , PM ₁₀ , NMVOC, SO ₂	ALL	ALL	ALL	ALL
HTAP_7: Waste	N/A	ALL	BC, OC, NO _x , NH ₃ , CO, PM _{2.5} , PM ₁₀ , NMVOC, SO ₂	ALL	ALL	ALL	ALL	ALL
HTAP_8.1: Agricultural waste burning	N/A	ALL	BC, OC, NO _x , NH ₃ , CO, PM _{2.5} , PM ₁₀ , NMVOC, SO ₂	ALL	N/A	ALL	ALL	ALL
HTAP_8.2: Agriculture livestock	NO _x , NH ₃ , PM ₁₀ , PM _{2.5} , NMVOC	NO _x , NH ₃ , PM ₁₀ , PM _{2.5} , BC, OC, NMVOC	NO _x , NMVOC, NH ₃ , PM ₁₀ , PM _{2.5} , OC	NO _x , NH ₃ , PM ₁₀ , PM _{2.5} , OC, NMVOC	NO _x , NH ₃ , PM ₁₀ , PM _{2.5} , BC, OC, NMVOC	NO _x , NH ₃ , PM ₁₀ , PM _{2.5} , BC, OC, NMVOC	NO _x , NH ₃ , PM ₁₀ , PM _{2.5} , OC, NMVOC	NO _x , NH ₃ , PM ₁₀ , PM _{2.5} , NMVOC
HTAP_8.3: Agriculture crops	NO _x , NH ₃ , PM ₁₀ , PM _{2.5}	NO _x , NH ₃ , PM ₁₀ , PM _{2.5} , BC, OC	NO _x , NH ₃ , PM ₁₀ , PM _{2.5}	NO _x , NH ₃ , PM ₁₀ , PM _{2.5}	NO _x , NH ₃ , PM ₁₀ , PM _{2.5} , BC, OC, NMVOC	NO _x , NH ₃ , CO, PM ₁₀ , PM _{2.5} , BC, OC, NMVOC, SO ₂	NO _x , NH ₃ , CO, PM ₁₀ , PM _{2.5} , OC, NMVOC, SO ₂	NO _x , NH ₃ , PM ₁₀ , PM _{2.5}

gap-filling information included using the EDGARv8.1 data. Table 4 reports a summary of the main features all previous HTAP emission mosaics in comparison with HTAP_v3.2, showing the advancements achieved with this work. The high sector disaggregation available within the HTAP_v3.2 mosaic gives needed flexibility to modellers to include or exclude emission sub-sectors in their simulations, in particular when integrating the anthropogenic emissions provided by HTAP_v3.2 with other components (e.g. natural emissions, forest fires, etc.). However, we recommend particular caution when using a natural emissions model such as MEGAN (Model of Emissions of Gases and Aerosols from Nature, <https://www2.acom.ucar.edu/modeling/model-emissions-gases-and-aerosols-nature-megan>, last access: 27 October 2025), which includes the estimation of NMVOC emissions from crops and soil NO_x emissions (including agricultural soils) that are also provided by the HTAP_v3.2 mosaic.

2.3 Inventory overviews

In the following sub-sections, details are provided on each officially reported inventory used to construct the HTAP_v3.2 emission mosaic.

2.3.1 CAMS-REG-v6.1 inventory

The CAMS-REG emission inventory was developed to support air pollutant and greenhouse gas modelling activities at the European scale. The inventory builds largely on the official reported data to the UN Framework Convention on Climate Change (UNFCCC) for greenhouse gases (for CO₂ and CH₄), and the Convention on Long-Range Transboundary Air Pollution (CLRTAP) for air pollutants. For the latter, data are collected for NO_x, SO₂, CO, NMVOC, NH₃, PM₁₀ and PM_{2.5}, including all major air pollutants. For each of these pollutants, the emission data are collected at the sector level at which these are reported for the time series 2000–2020 for each year and country. The CAMS-REG inventory covers UNECE-Europe, extending eastward until 60° E, therefore including the European part of Russia. For some non-EU countries, the reported data are found to be partially available or not available at all. In other cases, the quality of the reported data is found to be insufficient, i.e. with important data gaps or following different formats or methods. In this case, emission data from the International Institute for Applied Systems Analysis (IIASA) Greenhouse Gas – Air Pollution Interactions and Synergies (GAINS) model instead (IIASA, 2018) are used. This model is the main tool used to underpin pan-European and EU level air quality policies such as the UNECE Convention on Long Range Transboundary Air Pollution (UNECE, 2012) and the EU National Emission reduction Commitments Directive (European Commission, 2016).

After collecting all the emission data from the official inventory and the GAINS model, the source sectors are harmonised, distinguishing around 250 different subsectors. Some further changes are made to increase consistency, including (1) the use of bottom-up estimates for inland shipping given the differences in the way how these are estimated for individual countries, (2) replacement of reported emissions for agricultural waste burning with consistent estimates based on the Global Fire Assimilation System (GFAS) product (Kaiser et al., 2012) and (3) removal of NO_x from agricultural activities to prevent possible double counting with soil-NO_x estimates in modelling studies. For each detailed sector, a speciation is applied to the PM_{2.5} and PM₁₀ emissions, distinguishing elemental carbon (representing BC in the HTAP_v3.2 inventory), organic carbon and other non-carbonaceous substances for both the coarse (2.5–10 µm) and fine (< 2.5 µm) mode.

A consistent spatial resolution is applied across the entire domain, where a specific proxy is selected for each subsector to spatially distribute emissions, including for instance the use of point source emissions, e.g., from the European Pollutant Release and Transfer Register (E-PRTR), complemented with additional data from the reporting of EU Large Combustion Plants (European Commission, 2001) and the Platts/WEPP commercial database for power plants (Platts, 2017). Road transport emissions are spatially disaggregated using information from OSM (Open Street Map, 2017), combined with information on traffic intensity in specific road segments from OTM (OpenTransportMap, 2017). Agricultural livestock emissions are spatially distributed using global gridded livestock numbers (FAO, 2010). Furthermore, the Coordination of Information on the Environment (CORINE) land cover (Copernicus Land Monitoring Service, 2016) and population density are other key spatial distribution proxies.

After having spatially distributed the data, the ~250 different source categories are aggregated to fit with the HTAP_v3.2 sector classification (Table S1). Compared to the regular CAMS-REG sectors an additional split was made for agriculture other (GNFR L) where agricultural waste burning has been included as a separate source. On the other hand, road transport exhaust emissions, which are split to fuel type in the regular CAMS-REG inventory, were aggregated in one category. CAMS-REG-v6.1 is an update of an earlier versions (such as v4.2 which is described in detail in Kuenen et al., 2022) and based on the 2022 submissions of European countries, covering the years 2000–2020. While the official version of CAMS-REG-v6.1 only covers 2019–2020, underlying data have been prepared from 2000 onwards, similar to CAMS-REG versions 4 and 5. Additionally for HTAP_v3.2 a tailor-made version of the inventory was made to support the specific scope of the HTAP_v3.2 inventory in terms of years, pollutants and sectors.

The data are provided as gridded annual totals at a resolution of 0.05° × 0.1° (lat-lon), which implies that they can

Table 4. Main features of the different HTAP mosaics.

	HTAP_v1	HTAP_v2.2	HTAP_v3	HTAP_v3.2
Time coverage	2000–2005	2008 and 2010	2000–2018	2000–2020
Time resolution	yearly	yearly and monthly	yearly and monthly	yearly and monthly
Substances	CH ₄ , NMVOC, CO, SO ₂ , NO _x , NH ₃ , PM ₁₀ , PM _{2.5} , BC, OC	SO ₂ , NO _x , CO, NMVOC, NH ₃ (only for agriculture), PM ₁₀ , PM _{2.5} , BC, OC	SO ₂ , NO _x , CO, NMVOC, NH ₃ , PM ₁₀ , PM _{2.5} , BC, OC	SO ₂ , NO _x , CO, NMVOC, NH ₃ , PM ₁₀ , PM _{2.5} , BC, OC
Sectors	Aircraft, Ships, Energy, Industry Processes, Ground Transport, Residential, Solvents, Agriculture, Agriculture Waste Burning, and Waste	Air, Ships, Energy, Industry, Transport, Residential (including waste), and Agriculture (only for NH ₃)	International Shipping, Domestic Shipping, Domestic Aviation, International Aviation, Energy, Industry, Fugitives, Solvent Use, Road Transport, Brake and Tyre Wear, Other Ground Transport, Residential, Waste, Agricultural Waste Burning, Livestock, and Agricultural Crops	International Shipping, Domestic Shipping, Domestic Aviation (Take-off/Landing, Climbout /Descending, Cruise), International Aviation (Take-off/Landing, Climbout/Descending, Cruise), Energy, Industry, Fugitives, Solvent Use, Road Transport, Brake and Tyre Wear, Other Ground Transport, Residential, Waste, Agricultural Waste Burning, Livestock, and Agricultural Crops
Geographical coverage	Globe	Globe	Globe	Globe
Spatial resolution	0.1° × 0.1°	0.1° × 0.1°	0.1° × 0.1°	0.1° × 0.1°
Input datasets	UNFCCC, REAS, GAINS, EMEP, EPA, EDGARv4.1	US EPA, Environment Canada, MICS, TNO/EMEP Europe (MACC II), MICS Asia III+ REAS2.1, EDGARv4.3	CAMS-REG-v5.1, REASv3.2.1, US EPA, ECCC, CAPSS-KU, JAPAN (PM _{2.5} EI and J-STREAM), EDGARv6.1	CAMS-REG-v6.1, REASv3.2.1, US EPA, ECCC, CAPSS-KU, JAPAN (PM _{2.5} EI and J-STREAM), MEICv1.4, EDGARv8.1
Reference	Janssens-Maenhout et al. (2012)	Janssens-Maenhout et al. (2015)	Crippa et al. (2023)	This work

be easily aggregated to fit with the 0.1° × 0.1° resolution of the HTAP_v3.2 inventory. Along with the grids, additional information is available including height profiles as well as temporal profiles to break down the annual emissions into hourly data (monthly profiles, day-of-the-week profiles and hourly profiles for each day). Furthermore, the CAMS-REG inventory provides dedicated speciation profiles for NMVOC per year, country and sector.

2.3.2 US EPA inventory

Emissions estimates for the United States were based primarily on estimates produced for the EPA's Air QUALITY TimE Series Project (EQUATES), which generated a consistent set of modelled emissions, meteorology, air quality, and

pollutant deposition for the United States spanning the years 2002 through 2019 (<https://www.epa.gov/cmaq/equates>, last access: 27 October 2025, Foley et al., 2023). For each sector, a consistent methodology was used to estimate emissions for each year in the 18-year period, in contrast to the evolving methodologies applied in the triennial U.S. National Emissions Inventories (NEIs) produced over that span. The HTAP_v3.2 time series were extended back two years to 2000 using country, sector, and pollutant specific trends from EDGARv8.1. The 2020 NEI was used for the emission estimates for 2020. Because of the unique nature of 2020, it was not used to back cast any of the previous years.

Emissions estimates were calculated for more than 8000 Source Classification Codes grouped into 101 sectors and

Table 5. Main updates of emission input data of HTAP_v3.2 for each data provider compared to HTAP_v3.

Data provider	Major changes compared to HTAP_v3
REAS v3.2.1	No major changes.
CAPSS-KU	No major changes.
MEICv4.1	New data for China mainland.
JAPAN	Update of road transport emissions, and added off-road vehicles emissions. Re-evaluation of emission factors of stationary combustion sources. Extended time series up to 2020.
ECCC	Extended time series.
US EPA	Extended time series, removed fugitive dust emissions from the base emission maps.
CAMS-REG-v6.1	1. Use of country reported data based on 2022 inventory submissions and based on this extension of the time series up to 2020, 2. Use of updated point source data based on new Industrial Reporting database from the European Environment Agency, 3. Consistent inclusion of condensable organics in PM and its components (BC & OC) for small combustion.
EDGARv8.1	New spatial proxies, updated SO ₂ emissions from shipping, extended time series up to 2020.

then aggregated to the 16 HTAP_v3.2 emission sectors. The 2017 NEI (U.S. Environmental Protection Agency, 2021b) served as the base year for the time series. For each sector, emissions estimates were generated for previous years using one of four methods: (1) applying new methods to create consistent emissions for all years, (2) scaling the 2017 NEI estimates using annual sector-specific activity data and technology information at the county level, (3) using annual emissions calculated consistently in previous NEIs and interpolating to fill missing years, and (4) assuming emissions were constant at 2017 levels. The assumption of constant emissions was applied to a very limited number of sources. Foley et al. (2023) provides a detailed explanation of the assumptions used for each sector.

Emissions from electric generating units were estimated for individual facilities, combining available hourly emissions data for units with continuous emissions monitors (CEMs) and applying regional fuel-specific profiles to units without CEMS. On-road transport and non-road mobile emissions were estimated using emission factors from the MOTO Vehicle Emission Simulator (MOVES) v3 model (U.S. Environmental Protection Agency, 2021a). A complete MOVES simulation was completed only for the NEI years with national adjustment factors applied for years plus or minus one from the NEI year. For California, emission factors for all on-road sources for all years were based on the California Air Resources Board Emission Factor Model (EMFAC) (<https://ww2.arb.ca.gov/our-work/programs/mobile-source-emissions-inventory/>, last access: 27 October 2025). New non-road emissions estimates for Texas were provided by the Texas Commission on Environmental Quality. Emissions from oil and gas exploration and production were calculated using point source specific data

and the EPA Oil and Gas Tool (U.S. Environmental Protection Agency, 2021b), incorporating year-specific spatial, temporal, and speciation profiles. Residential wood combustion estimates were developed with an updated methodology incorporated into the 2017 NEI and scaled backward to previous years using a national activity as a scaling factor. Solvent emissions were estimated using the Volatile Chemical Product (VCPy) framework of Seltzer et al. (2021). Emissions from livestock waste were calculated with revised annual animal counts to address missing data and methodological changes over the period. Emissions for agricultural burning were developed using a new suite of activity data with the same methodology and input data sets from 2002 onwards. County-level estimates were only available for 2002 because activity data based on satellite information was not yet available. Emissions for forest wildfires, prescribed burns, grass and rangeland fires were also calculated in EQUATES but not included in the HTAP_v3.2 data. EQUATES also included fugitive dust emissions (e.g., unpaved road dust, coal pile dust, dust from agricultural tilling) and reduced their inventory values to account for the effects precipitation and snow cover by grid cell. These adjustments decreased annual PM₁₀ emissions by about 75 % on average. For use in HTAP, however, no meteorological adjustments were applied to fugitive dust emissions. These fugitive dust emissions were included in the previous version of this dataset (HTAP_v3), but are now not included in the base HTAP_v3.2 mosaic, as wind-blown fugitive dust emissions are not included in the estimates for other regions in either the HTAP_v3 or HTAP_v3.2 mosaics. Wind-blown fugitive dust emissions are available as a separate file for the US.

Non-point source emissions were allocated spatially based on a suite of activity surrogates (e.g. population, total road

miles, housing, etc.), many of which are sector specific. The spatial allocation factors were calculated for the EDGARv6.1 0.1° grid with no intermediate re-gridding. The spatial allocation factors were based on the same data as used for the EPA NEI 2017 and were held constant for the entire time series except for oil and gas sectors which were year-specific.

Emissions from the US EPA inventory were provided from 2002–2020 (Table 1). Emissions for the years 2000 and 2001 were estimated applying country, sector and pollutant specific trends from EDGAR to complete the entire time series. Table S1 provides an overview about the US EPA inventory sector mapping to the HTAP_v3.2 sectors.

2.3.3 Environment and Climate Change Canada (ECCC) inventory

The Canadian emissions inventory data were obtained from 2018 and 2021-released edition of Canada's Air Pollutant Emissions Inventory (APEI) originally compiled by the Pollutant Inventories and Reporting Division (PIRD) of Environment and Climate Change Canada (ECCC) (APEI, 2018) and (APEI 2021) respectively. Years 2000–2016 were based on (APEI, 2018) with three additional years (2017–2019) based on (APEI, 2021). Due to methodology changes, there is a slight discontinuity between (2000–2016) and (2017–2019) emissions as they come from different APEI releases.

This inventory contains a comprehensive and detailed estimate of annual emissions of seven criteria air pollutants (SO_2 , NO_x , CO, NMVOC, NH_3 , PM_{10} , $\text{PM}_{2.5}$) at the national and provincial/territorial level for each year for the period from 1990 to 2019. The APEI inventory was developed based on a bottom-up approach for facility-level data reported to the National Pollutant Release Inventory (NPRI) (APEI, 2021), as well as an in-house top-down emission estimates based on source-specific activity data and emissions factors. In general, methodologies used to estimate Canadian emissions are consistent with those developed by the U.S. EPA (US EPA, 2009) or those recommended in the European emission inventory guidebook (EMEP/EEA, 2013). These methods are often further adjusted by PIRD to reflect the Canadian climate, fuels, technologies and practices.

To prepare emissions in the desired HTAP classification, the APEI sector emissions were first mapped to the UNECE Nomenclature for Reporting (NFR) categories, which involved dividing the sector emissions into their combustion and process components. The NFR categories were then mapped to the HTAP 16 sector categories provided in the sector disaggregation scheme guide. Table S1 provides an overview of ECCC sector mapping to the HTAP_v3.2 sectors.

The HTAP-grouped APEI inventory emissions files were further processed by the Air Quality Policy-Issue Response (REQA) Section of ECCC to prepare the air-quality-modelling version of inventory files in the standard format (i.e., FF10 format) supported by the U.S EPA emissions pro-

cessing framework. To process emissions into gridded, speciated and total monthly values, a widely-used emissions processing system called the Sparse Matrix Operator Kernel Emissions (SMOKE) model, version 4.7 (UNC, 2019) was used. As part of the preparation for SMOKE processing, a gridded latitude-longitude North American domain at $0.1 \times 0.1^\circ$ resolution was defined with 920 columns and 450 rows covering an area of -142 to -50° W and 40 to 85° N. The point-source emissions in the APEI include latitude and longitude information so those sources were accurately situated in the appropriate grid cell in the Canadian HTAP gridded domain. However, to allocate provincial-level non-point source emissions into this domain, a set of gridded spatial surrogate fields was generated for each province from statistical proxies, such as population, road network, dwellings, crop distributions, etc. Over 80 different surrogate ratio files were created using the 2016 Canadian census data obtained from Statistics Canada website (<https://www12.statcan.gc.ca/census-recensement/2016/index-eng.cfm>, last access: 27 October 2025) and other datasets, such as the Canadian National Road Network (<https://open.canada.ca/data/en/dataset/3d282116-e556-400c-9306-ca1a3cada77f>, last access: 27 October 2025).

To map the original APEI inventory species to the HTAP's desired list of species, PM speciation profiles from the SPECIATE version 4.5 database (US EPA, 2016) were used to calculate source-type-specific EC and OC emissions. As a final step in SMOKE processing, the monthly emissions values were estimated using a set of sector-specific temporal profiles developed and recommended by the U.S. EPA (Sassi et al., 2021). For the point sources the NPRI annually reported monthly emissions proportions were applied. Emissions for the year 2020 were calculated by applying sector- and pollutant-specific trends from EDGAR.

2.3.4 REAS v3.2.1 inventory

The Regional Emission inventory in ASia (REAS) series have been developed for providing historical trends of emissions in the Asian region including East, Southeast, and South Asia. REASv3.2.1, the version used in HTAP_v3.2, runs from 1950 to 2015. REASv3.2.1 includes emissions of SO_2 , NO_x , CO, NMVOCs, NH_3 , CO_2 , PM_{10} , $\text{PM}_{2.5}$, BC, and OC from major anthropogenic sources: fuel combustion in power plant, industry, transport, and domestic sectors; industrial processes; agricultural activities; evaporation; and others. Emissions from REAS were included in the HTAP_v3.2 global mosaic inventory except for the geographical areas of China, Japan, and South Korea, for which the respective national inventories were used.

Emissions from stationary fuel combustion and non-combustion sources are traditionally calculated using activity data and emission factors, including the effects of control technologies. For fuel consumption, the amount of energy consumption for each fuel type and sector was obtained from

the International Energy Agency World Energy Balances, with the exception of Bhutan, Afghanistan, Maldives, Macau where UN Energy Statistics Database were used. Other activity data such as the amount of emissions produced from industrial processes were obtained from related international and national statistics. For emission factors, those without effects of abatement measures were set and then, effects of control measures were considered based on temporal variations of their introduction rates. Default emission factors and settings of country- and region-specific emission factors and removal efficiencies were obtained from scientific literature studies as described in Kurokawa and Ohara (2020) and references therein.

Emissions from road transport were calculated using vehicle numbers, annual distance travelled, and emission factors for each vehicle type. The number of registered vehicles were obtained from national statistics in each country and the World Road Statistics. For emission factors, year-to-year variation were considered by following procedures: (1) Emission factors of each vehicle type in a base year were estimated; (2) Trends of the emission factors for each vehicle type were estimated considering the timing of road vehicle regulations in each country and the ratios of vehicle production years; (3) Emission factors of each vehicle type during the target period were calculated using those of base years and the corresponding trends.

In REASv3.2.1, only large power plants were treated as point sources. For emissions from cement, iron, and steel plants, grid allocation factors were developed based on positions, production capacities, and start and retire years for large plants. Gridded emission data of EDGARv4.3.2 were used for grid allocation factors for the road transport sector. Rural, urban, and total population data were used to allocation emissions from the residential sector. For other sources, total population were used for proxy data.

For temporal distribution, if data for monthly generated power and production amounts of industrial products were available, monthly emissions were estimated by allocating annual emissions to each month using the monthly data as proxy. For the residential sector, monthly variation of emissions was estimated using surface temperature in each grid cell. If there is no appropriate proxy data, annual emissions were distributed to each month based on number of dates in each month.

Monthly gridded emission data sets at $0.25^\circ \times 0.25^\circ$ resolution for major sectors and emission table data for major sectors and fuel types in each country and region during 1950–2015 are available in text format from a data download site of REAS (<https://www.nies.go.jp/REAS/>, last access: 27 October 2025). Table S1 provides an overview about the REASv3.2.1 sector mapping to the HTAP_v3.2 sectors.

More details of the methodology of REASv3.2.1 are available in Kurokawa and Ohara (2020) and its supplement. (Note that REASv3.2.1 is the version after error corrections of REASv3.2 of Kurokawa and Ohara, 2020). Details of the

error corrections are described in the data download site of REAS.) For all countries covered by the REAS domain except China, Japan, and South Korea, the emissions were extended beyond 2015 by applying the sector, country, and pollutant specific trends from EDGAR.

2.3.5 CAPSS-KU inventory

In the Republic of Korea, the National Air Emission Inventory and Research Center (NAIR) estimates annual emissions of the air pollutants CO, NO_x, SO_x, TSP, PM₁₀, PM_{2.5}, BC, VOCs, and NH₃ via the Clean Air Policy Support System (CAPSS). The CAPSS inventory is divided into four source-sector levels (high, medium, low and detailed) based on the European Environment Agency's (EEA) CORE Inventory of AIR emissions (EMEP/CORINAIR). For activity data, various national- and regional-level statistical data collected from 150 domestic institutions are used. For large point sources, emissions are estimated directly using real-time stack measurements. For small point, area and mobile sources, indirect calculation methods using activity data, emission factors, and control efficiency are used.

Even though CAPSS (Clean Air Policy Support System) has been estimating annual emissions since 1999, some inconsistencies exist in the time series because of the data and methodological changes over the period. For example, emissions of PM_{2.5} were initiated from the year 2011 and not from 1999. Therefore, in the CAPSS emission inventory, PM_{2.5} emissions were calculated from 2011, and post-2011 the PM₁₀ to PM_{2.5} emission ratio was used to calculate the emissions from 2000 to 2010. These limitations make it difficult to compare and analyse emissions inter-annually. To overcome these limitations, re-analysis of the annual emissions of pollutants was conducted using upgrades of the CAPSS inventory, such as missing source addition and emission factor updates.

The biomass combustion and fugitive dust sector emissions from 2000 to 2014 were estimated and added in the inventory, which are newly calculated emission sources from 2015. As for the on-road mobile sector, new emission factors using 2016 driving conditions were applied from the year 2000 to 2015. Since the emissions from the combustion of imported anthracite coal were calculated only from 2007, the coal use statistics of imported anthracite from 2000 to 2006 were collected to estimate emissions for those years.

After all the adjustments, a historically re-constructed emissions inventory using the latest emission estimation method and data was developed. Table S1 provides an overview about the CAPSS sector mapping to the HTAP_v3.2 sectors.

2.3.6 JAPAN inventory (PM_{2.5}EI and J-STREAM)

The Japanese emission inventory contributing to the HTAP_v3.2 mosaic is jointly developed by the Ministry of

the Environment, Japan (MOEJ) for emissions arising from mobile sources and by the National Institute of Environmental Studies (NIES, 2022) for estimating emissions from fixed sources.

The mobile source emissions data for the HTAP_5.1, 5.2, and 5.4 sectors are based on the air pollutant emission inventory named “PM_{2.5} Emission Inventory” (PM_{2.5}EI, <https://www.env.go.jp/air/osen/pm/inventory.html>, last access: 27 October 2025). PM_{2.5}EI has been developed for the years 2012, 2015 and 2018 while for 2021 is currently under development. Almost all anthropogenic sources are covered, but emissions from vehicles are estimated in particular detail based on JATOP (Japan Auto-Oil Program) (Shibata and Morikawa, 2021). The emission factor of automobiles is constructed by MOEJ as a function of the average vehicle speed over several kilometres in a driving cycle that simulates driving on a real road. Emission factors are organized by 7 types of vehicles, 2 fuel types, 5 air pollutants, and regulation years, and have been implemented since 1997 as a project of MOEJ. By using these emission factors and giving the average vehicle speed on the road to be estimated, it is possible to estimate the air pollutant emissions per kilometre per vehicle. The hourly average vehicle speed of trunk roads, which account for 70 % of Japan’s traffic volume, is obtained at intervals of several kilometres nationwide every five years, so the latest data for the target year is used. For narrow roads, the average vehicle speed by prefecture measured by probe information is applied. It is 20 km h⁻¹ in Tokyo, but slightly faster in other prefectures. Starting emission is defined as the difference between the exhaust amount in the completely cold state and the warm state in the same driving cycle and is estimated by the times the engine started in a day. Chassis dynamometer tests are performed in a well-prepared environment, so for more realistic emissions estimates, temperature correction factor, humidity correction factor, deterioration factor, Diesel Particulate Filter (DPF) regeneration factor, and soak time correction factor are used. In addition to running and starting emissions, evaporative emissions from gasoline vehicles and non-exhaust particles such as road dust (including brake wear particles) and tire wear particles are combined to provide a vehicle emissions database with a spatial resolution of approximately 1 km × 1 km (30” arcsec latitude, 45” arcsec longitude), and a temporal resolution of an hour by month, including weekdays and holidays. Off-road vehicle emissions are estimated separately for 17 types of construction machinery, industrial machinery (forklifts), and 5 types of agricultural machinery. In all cases, emission factors by type and regulatory year per workload are used, as researched by the MOEJ. Although not as precise as automobiles, the off-road database is provided with the same temporal and spatial resolution as the automobile database.

Emissions from stationary sources in Japan are derived from the emission inventory developed in the Japan’s Study for Reference Air Quality Modelling (J-STREAM) model intercomparison project (Chatani et al., 2018, 2020, 2023).

In this emission inventory, emissions from stationary combustion sources are estimated by multiplying emission factors and activities including energy consumption, which is available in the comprehensive energy statistics. Large stationary sources specified by the air pollution control law need to report emissions to the government every three years. The emission factors and their annual variations were derived from the emissions reported by over 100 000 sources (Chatani et al., 2020). For fugitive VOC emissions, MOEJ maintains a special emission inventory to check progress on regulations and voluntary actions targeting 30 % reduction of fugitive VOC emissions starting from 2000. VOC emissions estimated in this emission inventory are used. Emissions from agricultural sources are consistent with the emissions estimated in the national greenhouse gas emission inventory (Center for Global Environmental Research et al., 2022). Emissions of all the stationary sources are divided into prefecture, city, and grid (approximately 1 × 1 km, 30” latitude, 45” longitude) levels based on spatial proxies specific to each source. Table S1 provides an overview about the Japanese inventory sector mapping to the HTAP_v3.2 sectors.

2.3.7 MEICv1.4 inventory

The Multi-resolution Emission Inventory for China (MEIC; <http://meicmodel.org.cn/>, last access: 27 October 2025), developed and maintained by Tsinghua University since 2010, provides high-resolution, multi-scale emission databases for anthropogenic air pollutants and greenhouse gases (Li et al., 2017; Zheng et al., 2018; Geng et al., 2024). The MEIC employs a technology-based approach to effectively capture the fast and complex evolution of technological operations in China. It encompasses 31 provinces across mainland China, incorporates over 700 anthropogenic emission sources, and covers key pollutants such as SO₂, NO_x, CO, NMVOCs, NH₃, PM₁₀, PM_{2.5}, BC, OC, and CO₂. The MEICv1.4 dataset (Geng et al., 2024) is used for the new HTAP_v3.2 global mosaic inventory, which spans from 1990 to 2020 and is publicly available at <http://meicmodel.org.cn/> (last access: 27 October 2025).

Emissions in MEIC are calculated using activity rates, unabated emission factors, penetration rates of manufacturing and pollution control technologies, and removal efficiencies of these technologies. Energy consumption data, categorized by fuel type, sector, and province, are derived from the China Energy Statistical Yearbook (<https://data.stats.gov.cn/>, last access: 27 October 2025). Industrial production data, segmented by product type and province, are sourced from other governmental statistics (<https://data.stats.gov.cn/>, last access: 27 October 2025). The distribution of combustion and processing technologies across sectors and industries is taken from the Ministry of Ecology and Environment (MEE) (unpublished data, referred to as the MEE database), which compiles plant-level information collected by local agencies and

verified by the MEE. Unabated emission factors are based on a broad spectrum of studies (Li et al., 2017). The net emission factors for specific fuels/products within sectors evolve dynamically due to rapid technological adoption, necessitating a technology-based methodology to monitor these changes. Penetration rates for various technologies are sourced from extensive statistics (Li et al., 2017) and the MEE database.

Sector-specific emission models underpin the MEIC framework. For coal-fired power plants, emissions are calculated using detailed unit-level data on activity rates, emission factors, control technology progress, operation status, and geographic location, enabling the tracking of changes at the unit level (Liu et al., 2015; Tong et al., 2018). Cement production emissions are similarly modeled at the unit level, accounting for operational status, clinker and cement production volumes, production capacity, facility commissioning/retirement dates, and control technologies (Liu et al., 2021). On-road vehicle emissions are estimated using vehicle stock and monthly emission factors at the county level, as well as fleet turnover data at the provincial level, capturing spatial and temporal variations in vehicle activity and emissions (Zheng et al., 2014). Residential sector emissions are derived using a survey-based model linking solid fuel consumption to heating degree days, income levels, coal production, coal prices, and vegetation coverage, correcting for underreported rural coal consumption and overestimated crop residue use in official statistics (Peng et al., 2019).

Monthly emissions are allocated from annual totals using source-specific monthly profiles, developed based on statistical data such as fuel consumption and industrial production. Spatial allocation employs geographic coordinates for power and cement facilities, while spatial proxies like population density and road networks are used for mobile and diffuse sources to disaggregate provincial emissions to grid scales. Emissions are first mapped to a 1 km grid and subsequently aggregated to a 0.1° grid. Further details on the methodology of MEICv1.4 can be found in Geng et al. (2024) and its supplementary materials.

2.4 Gap-filling methodology with EDGARv8.1

EDGAR is a globally consistent emission inventory of air pollutant and greenhouse gases developed and maintained by the Joint Research Centre of the European Commission (<https://edgar.jrc.ec.europa.eu/>, last access: December 2024). The EDGAR methodology used to compute greenhouse gas and air pollutant emissions has been described in detail in several publications (Janssens-Maenhout et al., 2019; Crippa et al., 2018) and summarised here after. In EDGAR, air pollutant emissions are computed by making use of international statistics as activity data (e.g. International Energy Balance data, Food and Agriculture Organisation statistics, USGS Commodity Statistics), region- and/or country-specific emission factors by pollutant/sector, and technology and abatement measures, following Eq. (1)

$$EM_{i(C,t,x)} = \sum_{j,k} AD_{i(C,t)} \cdot TECH_{i,j(C,t)} \cdot EOP_{i,j,k(C,t)} \cdot EF_{i(C,t,x)} \cdot (1 - RED)_{i,j,k(C,t,x)} \quad (1)$$

where EM are the emissions from a given sector i in a country C accumulated during a year t for a chemical compound x , AD the country-specific activity data quantifying the human activity for sector i , TECH the mix of j technologies (varying between 0 and 1), EOP the mix of k (end-of-pipe) abatement measures (varying between 0 and 1) installed with a share k for each technology j , and EF the uncontrolled emission factor for each sector i and technology j with relative reduction (RED) by abatement measure k . Emission factors are typically derived from the EMEP/EEA Guidebooks (EMEP/EEA, 2013, 2019, 2016), the AP-42 (US EPA, 2009) inventory and scientific literature.

Annual country- and sector-specific air pollutant emissions are then disaggregated into monthly values (Crippa et al., 2020) and subsequently spatially distributed by making use of detailed proxy data (Janssens-Maenhout et al., 2019; Crippa et al., 2021a, 2024).

As the most comprehensive and globally consistent emission database, the latest update of the EDGAR air pollutant emissions inventory, EDGARv8.1 (https://edgar.jrc.ec.europa.eu/dataset_ap81, last access: December 2024), is used in the HTAP_v3.2. mosaic to complete missing information from the officially reported inventories, as reported in Table 3. In addition of using the latest international statistics as input activity data for computing emissions (e.g. IEA, 2022; FAOSTAT, 2023, etc.), EDGARv8.1 includes important updates compared to previous versions for estimating air pollutant emissions, such as the improvement of road transport emission estimates for many world regions (refer to Lekaki et al., 2024) and updated technologies, abatement measures and emission factors for power plant emissions and residential emissions in Europe.

EDGARv8.1 incorporates new spatial proxies used to distribute national emissions by sector over the globe (Crippa et al., 2024) and new monthly profiles for the residential sector making use of heating degree days using ERA-5 temperature data. SO₂ emissions from international and domestic shipping have been revised including the revision of the sulphur content of the fuel following the International Maritime Organisation (IMO) studies (Smith et al., 2015; Faber et al., 2020) and scientific literature (Diamond, 2023; Osipova et al., 2021). In the Supplement (Sect. S2), the assessment of EDGAR emission data is reported in comparison with global and regional inventories.

3 Results

3.1 Annual time series analysis: trends and regional and sectoral contributions

Having a consistent set of global annual emission inventories for a two-decade period allows the investigation of global emissions trends for the inventory pollutants and regional and sectoral contributions. Figure 2 presents annual time series (2000–2020) of the global emissions of the nine air pollutants included in the HTAP_v3.2 mosaic separated into the actual contributions of 12 regions, while Fig. 3 presents the emission time series by sector and compound. Figure 4 shows the corresponding relative contributions of (a) 16 sectors and (b) 12 regions to the 2018 global emissions of these same pollutants. We can then discuss each pollutant in turn. In the following paragraphs we shortly present global and regional air pollutant emissions and their trends over the 2000–2020 period as provided by the HTAP_v3.2 data. Emissions are not presented with a confidence level since no comprehensive bottom-up uncertainty analysis has been performed in the context of the mosaic compilation, however see discussion in Sect. 3.5. Since 2020 emissions have been strongly influenced by the COVID-19 pandemic, some of the figures and results will refer to the year 2018 (also for comparability reasons with HTAP_v3).

Global SO₂ emissions declined from 98.9 to 58.3 Mt between 2000 and 2020. This decreasing pattern is found for several world regions with the fastest decline in Eastern Asia, where after the year 2005 SO₂ emissions began to decrease steadily. This is consistent with the use of cleaner fuels with lower sulphur content and the implementation of desulphurisation techniques in power plants and industrial facilities in China in accordance with the 11th Five-Year Plan (FYP, 2006–2010 (Planning Commission, 2008)) and the 12th Five-Year Plan (FYP, 2011–2015, Hu, 2016) (Sun et al., 2018). Similarly, industrialised regions, such as North America and Europe, are characterised by a continuous decreasing trend in SO₂ emission, which had started well before the year 2000 due to the implementation of environmental and air quality legislation (EEA, 2022). Increasing SO₂ emissions, on the other hand, are found for Southern Asia (+115 % in 2018 compared to 2000), South-East Asia and Pacific (+60.4 %), and Africa (+44.2 %). These increases mostly arise from the energy, industry, and (partly) residential sectors, and reflect the need for emerging and developing economies to mitigate these emissions. Emissions estimated using satellite retrievals and model inversions confirm the trends provided by the HTAP_v3.2 mosaic (Liu et al., 2018). SO₂ is mostly emitted by power generation and industrial activities, which in 2018 represent 42.6 % and 27.5 %, respectively, of the global total. Despite measures in some specific sea areas to mitigate sulphur emissions, globally they have been rising steadily with increasing activity. International shipping represents 11.9 % of global SO₂ emissions

in 2018 (and 4 % in 2020 due to the COVID-19 pandemic), and it is 21.9 % higher compared to the 2000 levels (Fig. 3).

Global NO_x emissions increased from 108.2 Mt in 2000 to 122.1 Mt in 2011 as a result of the increase in energy- and industry-related activities in particular over the Asian domain, and then started declining down to 113.6 Mt in 2018 due to the stabilisation and reduction of Chinese emissions. A further decline of global emissions down to 103 Mt in 2020 is found as consequence of the COVID-19 pandemic. On the opposite, historically industrialised countries show the strongest decreases in the emissions: –65.8 % for North America (in 2018 compared to 2000), –43.6 % for Europe –34.8 % for Australia, Japan, and New Zealand. Lower emission reductions are found for Eastern Europe and West-Central Asia (–8.9 %). Comparable spatio-temporal patterns are found by satellite OMI data and ground based measurements of NO₂ concentrations (Jamali et al., 2020). NO_x is mainly produced at high combustion temperatures (e.g., power and industrial activities, 35.1 % of the global total), but also by road transportation (26.6 % of the global total) and international shipping (14.8 % of the global total).

CO is mostly emitted by incomplete combustion processes from residential combustion, transportation and the burning of agricultural residues. Globally, CO emissions declined from 552.3 Mt in 2000 to 533.9 Mt in 2018 (and 515.5 Mt in 2020), with different regional trends. Historically industrialised regions have reduced their emissions over the years (–48.2 % in Europe and –63.1 % in North America), while CO emissions increased in Africa by 44.8 % and in Southern Asia by 54.5 %. Road transport CO emissions halved over the past two decades (–54.5 %), while the emissions from all other sectors increased. This trend can be explained by the effective implementation of regulatory standards on vehicles and, in particular, the widespread use and continuous improvement of three-way catalysts in gasoline vehicles since the early 1980s, as well as the more recent introduction of oxidation catalysts in diesel vehicles (Twigg, 2011). These results are consistent with MOPITT (Measurement of Pollution in the Troposphere) satellite retrievals, which mostly show the same trends over the different regional domains over the past decades (Yin et al., 2015).

NM VOC emissions increased from 116.1 Mt in 2000 to 146 Mt in 2018 (and 141.8 Mt in 2020). These emissions are mostly associated with the use of solvents (23 % of the 2018 global total), fugitive emissions (22.3 %), road transportation (including both combustion and evaporative emissions, 14.3 %) and small-scale combustion activities (19.9 %). The most prominent increases in the emissions at the global level are found for the solvents sector (+73.4 %). In 2018, NM VOC emissions from solvents were 5.3 and 4.5 times higher than in 2000 in China and India, respectively, while a rather stable trend is found for US and Europe.

Global NH₃ emissions increased from 43.3 Mt in 2000 to 55.3 Mt in 2018 (and 56.8 Mt in 2020) due to enhanced emissions from agricultural activities. In particular, NH₃

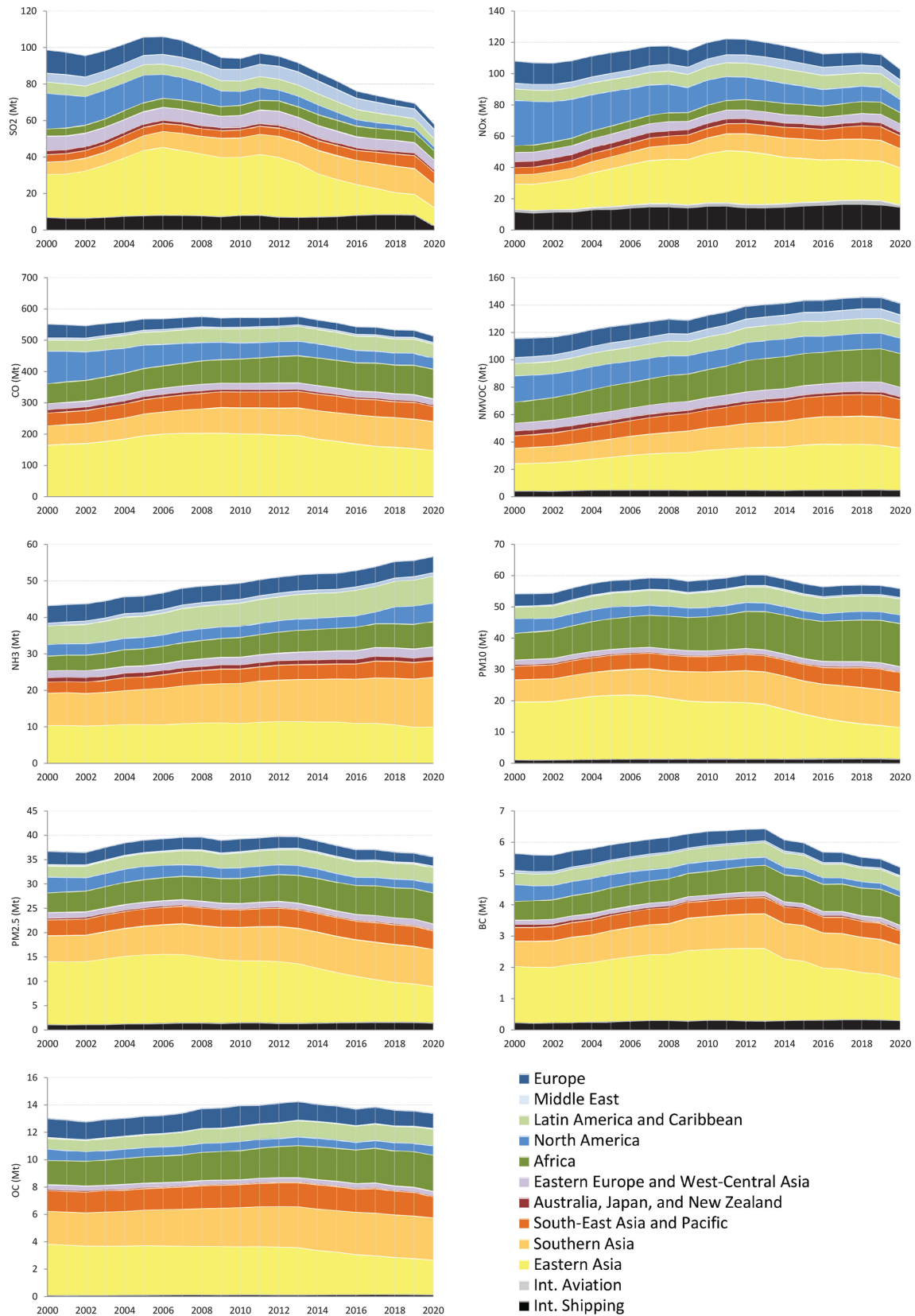


Figure 2. Time series of gaseous and particulate matter pollutants from HTAP_v3.2 by aggregated regions. Regional grouping follows the Intergovernmental Panel on Climate Change Sixth Assessment Report (IPCC AR6) definitions. Table S3 provides information on the country affiliations in the IPCC AR6 regions.

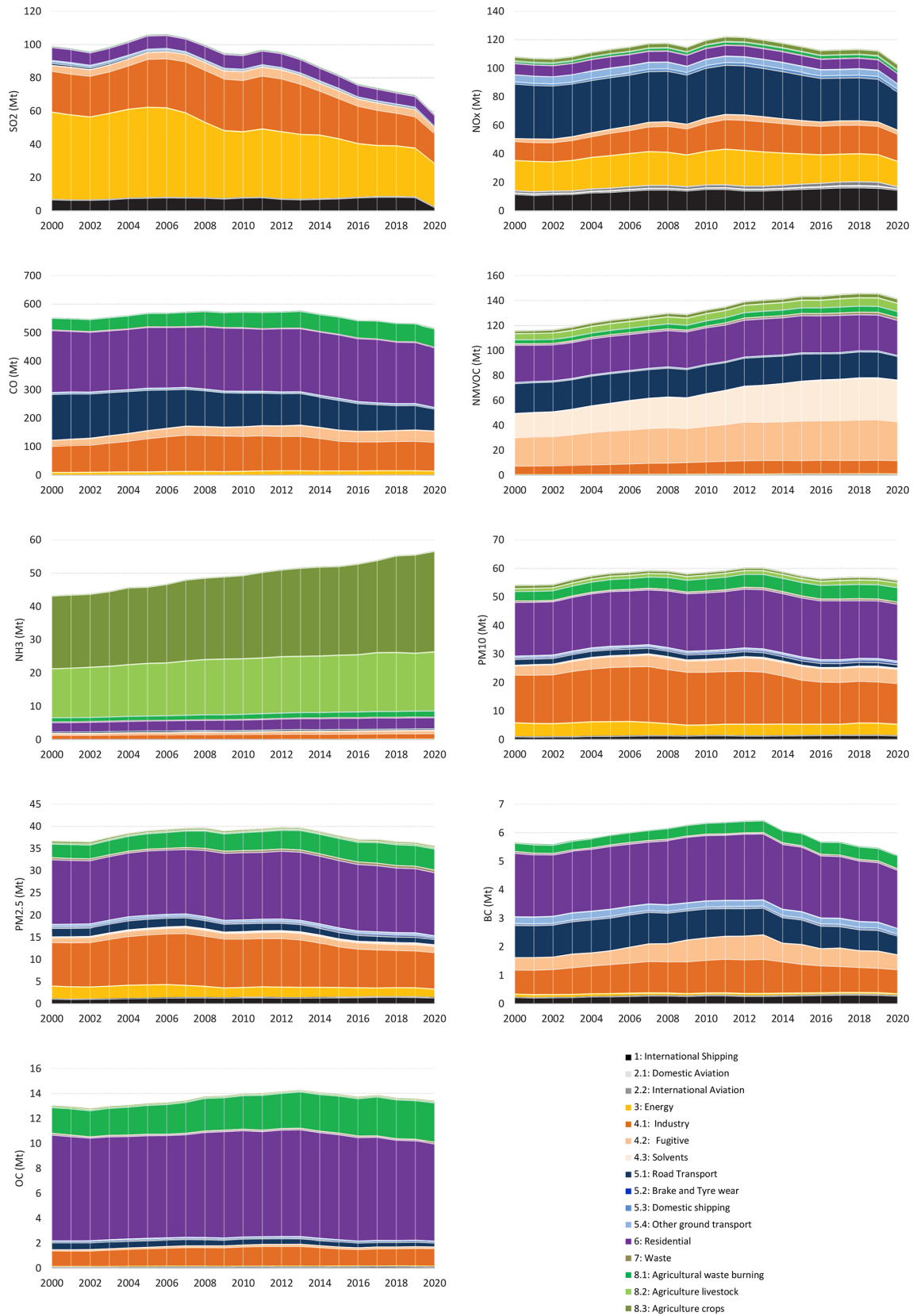


Figure 3. Time series of gaseous and particulate matter pollutants from HTAP_v3.2 by sector.

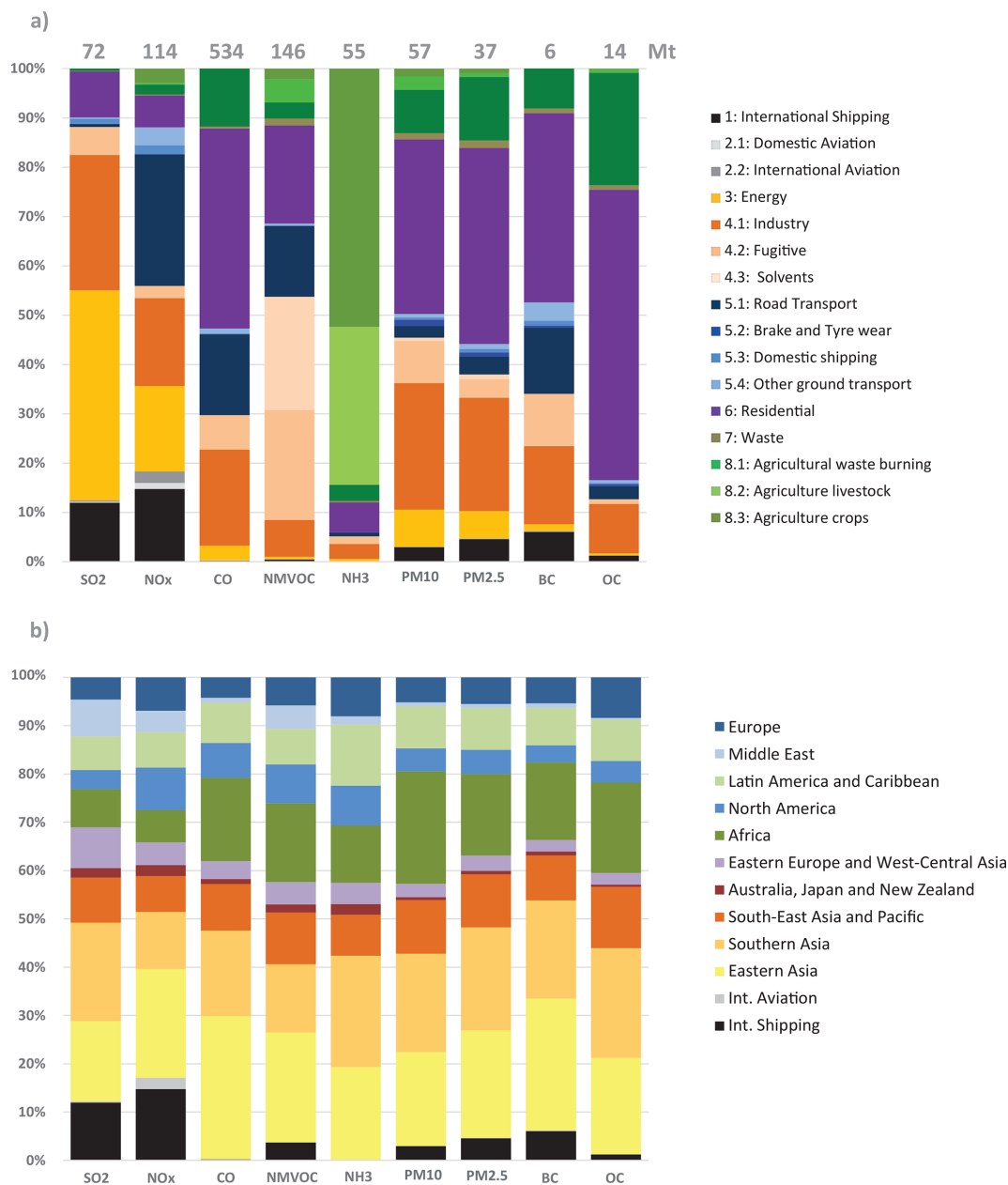


Figure 4. Sectoral (a) and regional (b) breakdown of air pollutant emissions from HTAP_v3.2 for the year 2018. At the top of each bar in panel (a), total emissions for each pollutant are reported (in Mt).

emissions strongly increased in Africa (+61.8% in 2018 compared to 2000), South-East Asia and Pacific (54.9%), Southern Asia (+44.4%), and Latin America and Caribbean (+36.8%).

Particulate matter emissions increased from 55.3 Mt PM₁₀ in 2000 to 59.9 Mt in 2018 (and 58.6 Mt in 2020) at the global level, with different regional trends: +65.9% for Southern Asia (in 2018 compared to 2000), +56.8% for Africa, +39.6% for Middle East, +33.1% for Latin America and Caribbean. These increases were mostly associated with increases in agricultural waste burning and the livestock, en-

ergy, and waste sectors. By contrast, Eastern Asia (−40.3%), North America (−22.9%), and Australia, Japan, and New Zealand (−33.5%) significantly decreased their PM₁₀ emissions over the past two decades due to the continuous implementation of reduction and abatement measures for the energy, industry, road transport and residential sectors (Crippa et al., 2016). The same regional emission trends and order of magnitude of emission changes as for PM₁₀ is also found for PM_{2.5}, BC and OC. In HTAP_v3, the relative contribution of North America to global PM₁₀ is quite high compared to other substances due to fugitive dust emissions (e.g., unpaved

road dust, coal pile dust, dust from agricultural tilling) which have not been adjusted for meteorological conditions (e.g., rain, snow) and near-source settling and mitigation (e.g., tree wind breaks) because these removal mechanisms are better addressed by the chemical transport models. Additional uncertainty may be therefore introduced for these emissions, depending on the modelling assumptions of each official inventory. Similarly, particulate matter speciation into its carbonaceous components is often challenging and subjected to higher level of uncertainty, for instance because different definitions are used for PM in inventories, including condensable emissions or not (Denier van der Gon et al., 2015). Improvement of the accuracy of such emissions (e.g. BC and OC emissions over the European domain) are included in this work compared to HTAP_v3.

The extension of the HTAP mosaic up to the year 2020 allows investigating the impact of COVID-19 pandemic on global, regional and sectoral pollutant emissions, as shown in Figs. 2 and 3. All pollutants sensibly decreased from 2019 to 2020 due to the restrictions and reduced activities induced by the COVID-19 pandemic. According to our study, the following emission reductions are found: -8.5% for NO_x (mostly due to a significant decrease in power generation, industrial and transportation emissions), -3.2% for CO, -2.8% for NMVOC, -1.9% and -2.1% for PM_{10} and $\text{PM}_{2.5}$, -4.6% for BC and -1.1% for OC. Only NH_3 shows an increasing trend by 1.9% due to the reduced impact of COVID-19 restriction on the agricultural sector. SO_2 emissions experienced a much larger decrease (-16.3%) not only due to the COVID-19 pandemic but mostly to the implementation of the International Maritime Organisation (IMO) regulations (IMO, 2014; IMO, 2020; Diamond, 2023; Osipova et al., 2021), which lowered the sulfur content in fuel and reduced SO_2 shipping emissions by 72% . From a sectoral perspective, international aviation emissions are those associated with the highest reduction (-52.3%) for all pollutants due to the flights restrictions, followed by the power generation sector with emission reductions between 4% and 10% depending on the pollutant and road transport sector (around -10%). These emission reductions are consistent with the sectoral emission decreases found in global studies for fossil CO_2 (Crippa et al., 2021b) which are directly linked to a reduction in anthropogenic combustion activities. From a regional perspective, a decrease from around 5% to 12% is found for all regions and combustion related pollutants.

3.2 Emission maps

Spatially distributed emission data describe where emissions take place, as input for local, regional and global air quality modelling. As noted in Sect. 2.2, nationally aggregated air pollutant emissions are spatially distributed over the corresponding national territory using spatial proxy data which are believed to provide a relatively good representation of where emissions take place. Depending on the emitting sec-

tor, air pollutants can be associated with the spatial distributions of point sources (e.g., in the case of power plant or industrial activities), road networks (e.g., for transportation related emissions), settlement areas (e.g., for small-scale combustion emissions), crop and livestock distribution maps, ship tracks etc. Using reliable and up-to-date spatial information to distribute national emissions is therefore relevant, although challenging. Multiple assumptions are often made by inventory compilers when developing their inventories, which may result in differences when analysing spatially distributed emissions provided by different inventory compilers over the same geographical domain.

One key goal of the HTAP_v3.2 mosaic is to collate in one inventory the most accurate spatially-distributed emissions for all air pollutants at the global level, based on the best available local information. Point sources related with emissions from power plant and industrial facilities represent one the most critical spatial information to be retrieved, and their misallocation can significantly affect the characterisation of local air quality. This challenge is also present in the HTAP_v3.2 mosaic. For example, the REASv3.2.1 inventory is still using limited information to distribute emissions from these two sectors especially for industrial plants. Depending on the region, point source information could be limited compared to datasets used in inventories of North America, Europe, and China. To overcome this issue, in HTAP_v3.2 MEIC data were integrated for China, but the participation of national emission inventory developers from India and other Asian countries is recommended for future updates. The impact can be seen in Fig. 5, which shows the global map of SO_2 emissions in 2018 based on the HTAP_v3.2 mosaic compilation, where information about the magnitude and the type of emission sources for the different regions can be retrieved. The energy and industry sectors contribute a large fraction of SO_2 emissions (Fig. 4a), but the spatial distribution of these emissions is qualitatively different in North America and Europe than in Asia (i.e., more “spotty”, less smooth and widely distributed). Ship tracks cover the entire geographical marine domain, consistent with emissions from the STEAM model (Jalkanen et al., 2012; Johansson et al., 2017) included in the EDGARv8.1 database, although showing marked emissions over the Mediterranean Sea, Asian domain, Middle East and North American coasts. Furthermore, emissions from power plant and industrial activities, as well as small-scale combustion are prominent over the Asian domain, Eastern Europe, and some African regions.

Sector-specific case studies are presented in the maps of Figs. 6–8. The year 2018 is represented in the maps instead of 2020 to exclude the peculiarities of the COVID-19 pandemic. Figure 6 shows the comparison of annual NO_x emissions for the year 2000 and 2018. The road transport sector is a key source of NO_x emissions (cf. Fig. 4), and this contribution is reflected in the visible presence of road networks in the maps. Decreasing emissions are found for industrialised regions (USA, Europe, Japan) thanks to the in-

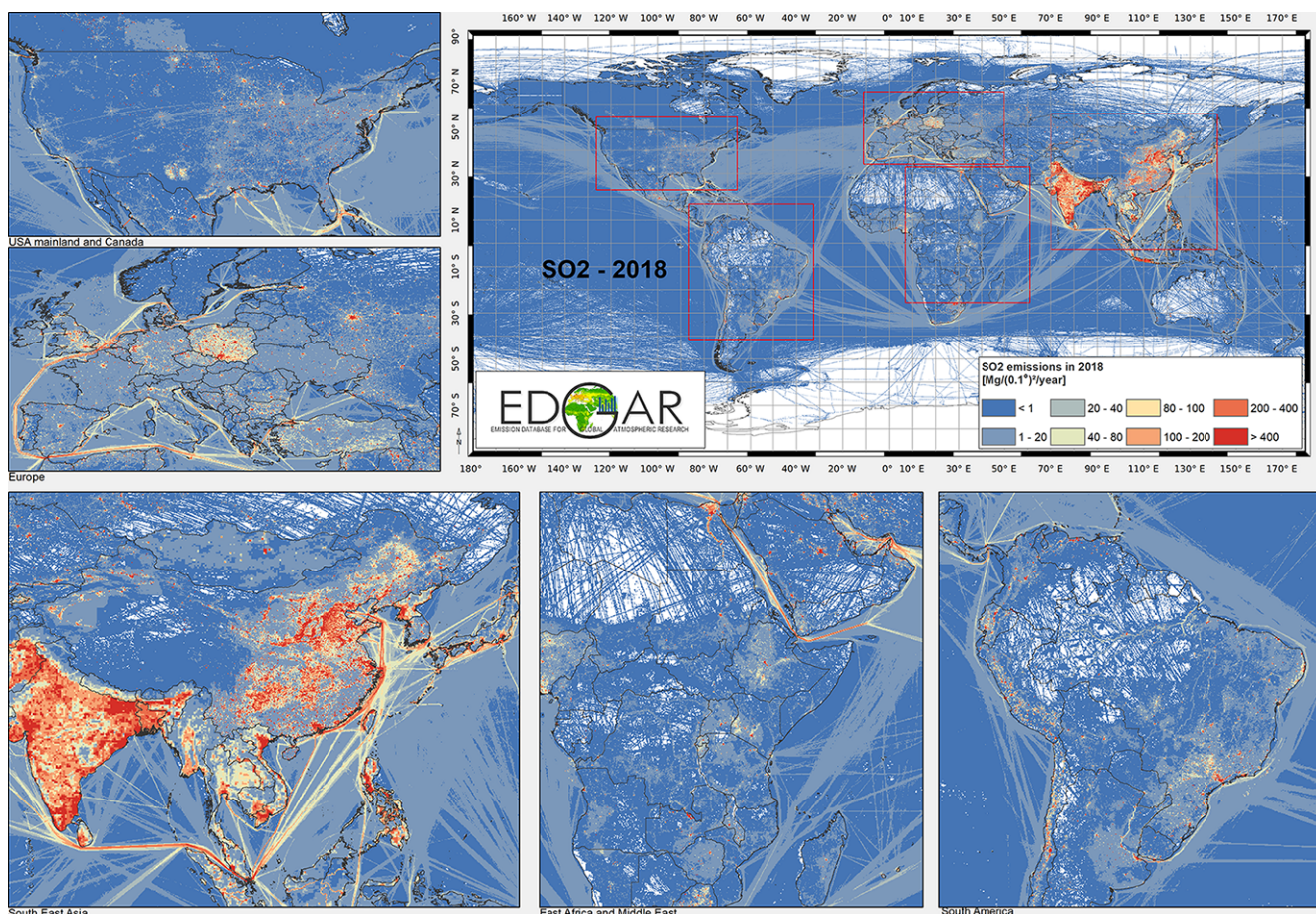


Figure 5. HTAP_v3.2 mosaic: SO₂ emission grid maps for the year 2018.

roduction of increasingly restrictive legislation on vehicle emissions since the 1990s, whereas a steep increase is found for emerging economies and in particular India, China, and the Asian domain. Figure 7 shows the different spatial allocation of PM_{2.5} emissions from the residential sector during the month of January 2018, with higher emission intensities evident in the Northern Hemisphere (cold season) and the lower values in the Southern Hemisphere (warm season). Figures 8 and 9 show the spatio-temporal allocation of agriculture-related emissions, and specifically, PM₁₀ emissions from agricultural waste burning and NH₃ emissions from agricultural soil activities, which are affected by strong regional seasonality as discussed more in detail in Sect. 3.3.

3.3 Monthly temporal distribution

3.3.1 Monthly variability by region

The magnitude of air pollutant emissions varies by month because of the seasonality of different anthropogenic activities and their geographical location (e.g., Northern vs. Southern Hemisphere regions). Figures 10 and 11 (and S18, S19 and S20) show the monthly distribution of regional emissions for

those pollutants and sectors for which higher variability is expected. The year 2015 was chosen since it is the last year for which all of the official data providers have data. Figure 10 shows monthly NH₃ emissions by region from three agricultural activities (agricultural waste burning, livestock, and crops). These sectors display the largest variability by month, reflecting the seasonal cycle and the region-specific agricultural practices, such as fertilisation, crop residue burning, manure and pasture management, animal population changes, etc. In Fig. 11, NO_x emissions from residential activities show a particular monthly distribution, with the highest emissions occurring during the cold months shifted for the Northern and Southern Hemispheres. By contrast, regions in the equatorial zone do not show a marked monthly profile even for residential activities. The energy sector also follows monthly-seasonal cycles related to the demand for power generation, which is also correlated with ambient temperature and local day length. Transport-related emissions do not show a large variation by month, whereas daily and weekly cycles for transport-related emissions, which are typically more relevant, are beyond the temporal resolution of this work.

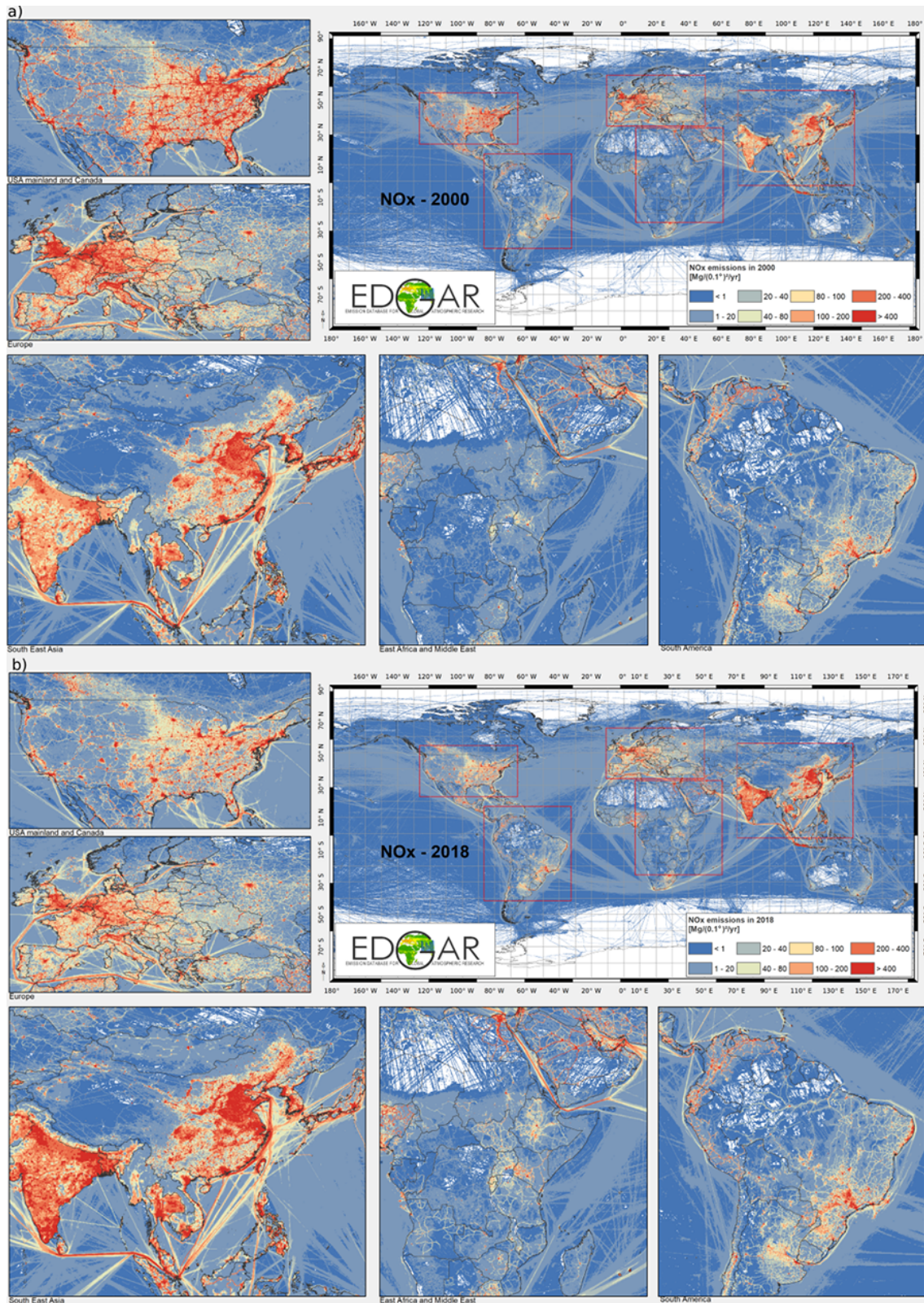


Figure 6. HTAP_v3.2 mosaic: NO_x emission grid maps in 2000 (a) and 2018 (b).

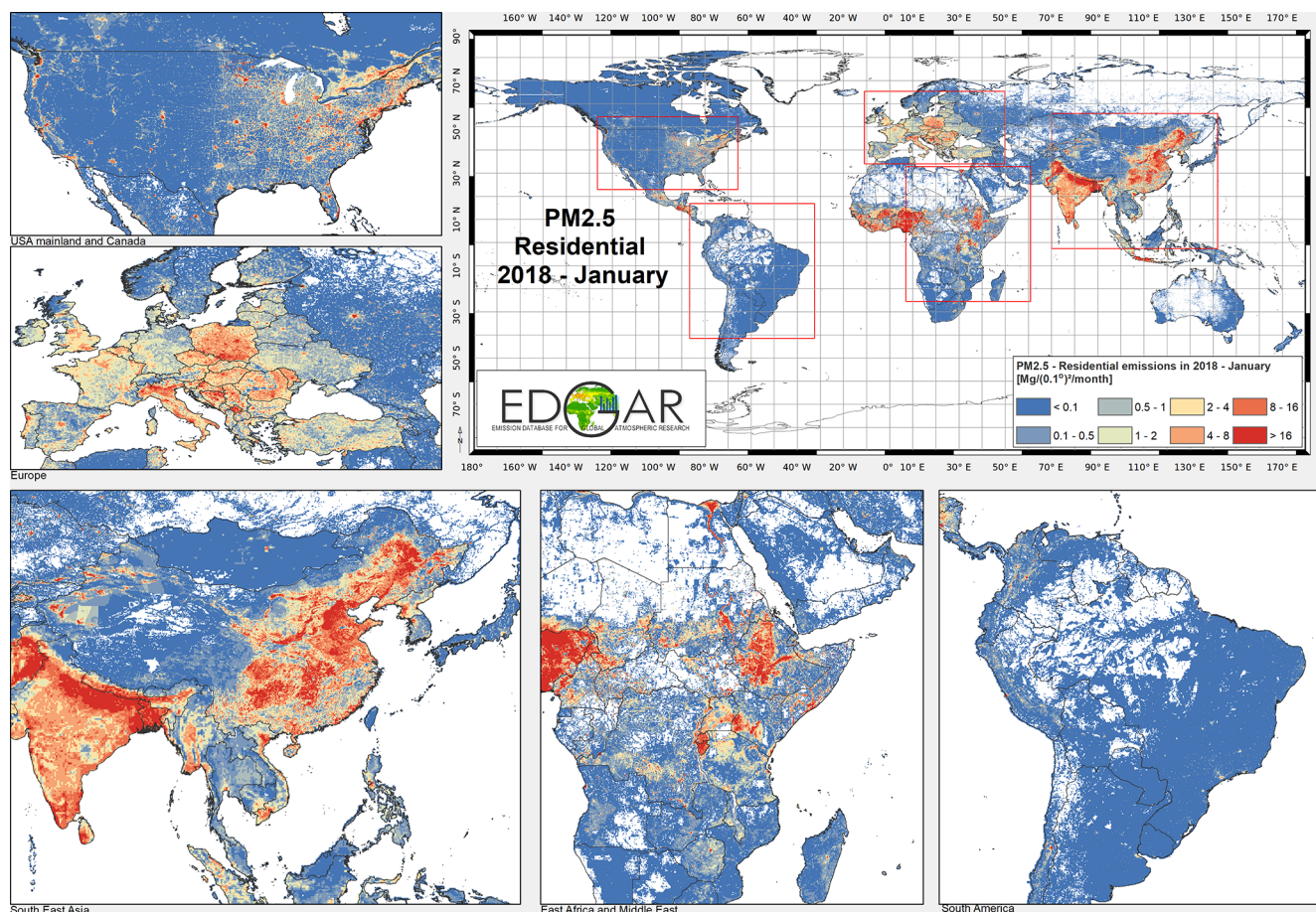


Figure 7. HTAP_v3.2 mosaic: PM_{2.5} emissions from residential activities in January 2018.

Although a spatio-temporal variability of the HTAP_v3.2 emissions is found in these figures, a more in-depth analysis reveals that with the exception of few regions and sectors (e.g., Canada, USA and regions gap-filled with EDGAR), no inter-annual variability of the monthly profiles is present, meaning that the majority of official inventories assume the same monthly distribution of the emissions for the past two decades (refer to Figs. S21–S26). This is different from the approach used for example by EDGAR (Crippa et al., 2020), ECCC for Canada, and U.S. EPA for the USA, where year-dependent monthly profiles are used for specific sectors, in particular for residential, power generation, and agricultural activities. Further analysis has shown that for the European domain regional rather than country-specific monthly profiles are applied. Therefore, for Europe new state-of-the-art profiles have been made available under the CAMS programme by Guevara et al. (2021).

3.3.2 Spatially-distributed monthly emissions

An important added value of HTAP_v3.2 comes from the availability of monthly gridmaps that reflect the seasonality of the emissions for different world regions. Access to spa-

tially distributed monthly emissions is essential to design effective mitigation actions, providing information on hot spots of emissions and critical periods of the year when emissions are highest.

Figure 12 shows mid-season PM_{2.5} monthly emissions arising from the residential sector in 2018. The global map shows higher emissions in the Northern Hemisphere during January, while the opposite pattern is found for the Southern Hemisphere in July. Agriculture is an important activity characterised by strong seasonal patterns, as shown in Figs. 13 and 14. Figure 14 shows PM₁₀ monthly emission maps from agricultural residue burning in 2018 from HTAP_v3.2, highlighting higher emissions over certain months of the year related with specific burning practices of agricultural residues for different world regions. For example, during the month of April, intense burning of crop residues is found in Africa (Nigeria, Ethiopia, Sudan, South Africa, etc.), South America (Brazil, Argentina, Colombia, etc.), Northern India, and South-Eastern Asia (e.g., Vietnam, Thailand, Indonesia, Philippines, etc.). Figure 13 represents the yearly variability of NH₃ emissions from agricultural soils activities, mostly related with fertilisation. During the spring months (March

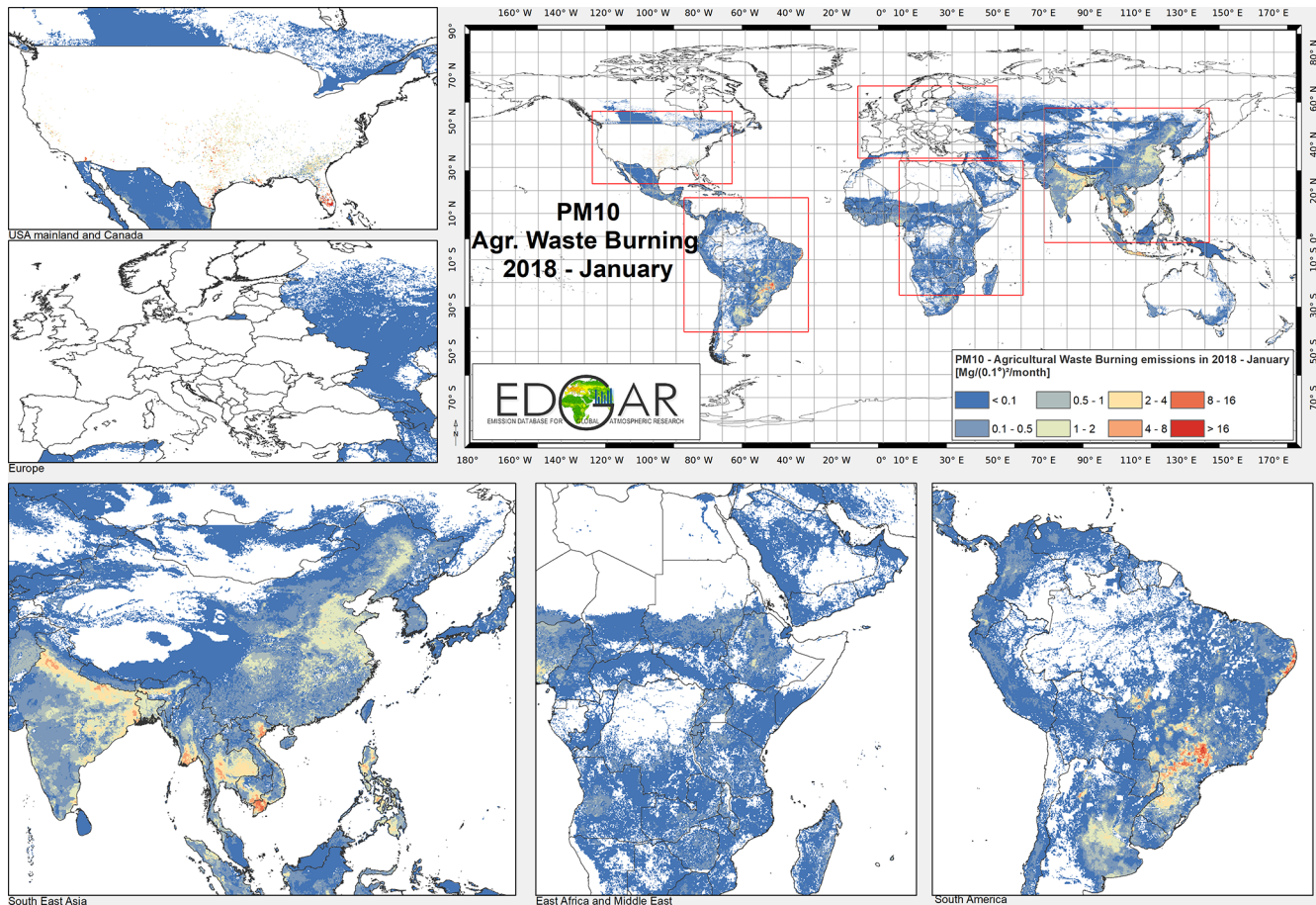


Figure 8. HTAP_v3.2 mosaic: PM₁₀ emissions from agricultural waste burning in January 2018.

and April), intense agricultural soils activities are found over Europe and North America compared to other months, while during the month of October the highest emissions are for this sector are found in China, India, several countries of the Asian domain, but also in USA, Australia, and Latin America. These results are consistent with satellite based observations performed using Cross-track Infrared Sounder (Shepherd et al., 2020).

3.4 Vertical distribution of the emissions

3.4.1 Aircraft emissions

In EDGARv8.1 the emissions are provided at three effective altitude levels (landing/take-off, ascent/descent, and cruising). The spatial proxy for the aviation sector is derived from International Civil Aviation Organization (ICAO, 2015) which specifies a typical flight pattern with landing/take-off cycle within few km of the airport, followed by climb-out/descending phase during the first 100 km and the last 100 km of a flight and finally the remaining part from 101 km until the last 101 km as the cruise phase. Routes and airport locations are taken from the Airline Route Mapper of ICAO

(2015). In HTAP_v3.2, aircraft emissions are provided as domestic and international, including information about the three altitude ranges in each case.

3.4.2 Speciation of NMVOC emissions

For emission data to be useful for modellers, total NMVOC emissions must be decomposed into emissions of individual NMVOC species. As the chemical mechanisms used by models can differ with respect to the NMVOC species they include, it is not practical to provide an NMVOC speciation which is usable by all models. Instead, a speciation is provided here for the set of 25 NMVOCs defined by Huang et al. (2017) and the corresponding data are made available on the HTAP_v3.2 website. The absolute values of 25-category speciated NMVOC emissions were obtained for all countries for the 28 EDGAR sectors from here: https://edgar.jrc.ec.europa.eu/dataset_ap432_VOC_spec (last access: 27 October 2025). The absolute NMVOC emissions of each species from each sector in this dataset were remapped to the HTAP_v3.2 sectors following the mapping from Table 2, then converted to a speciation by dividing by the total emissions of each individual species for the four world regions

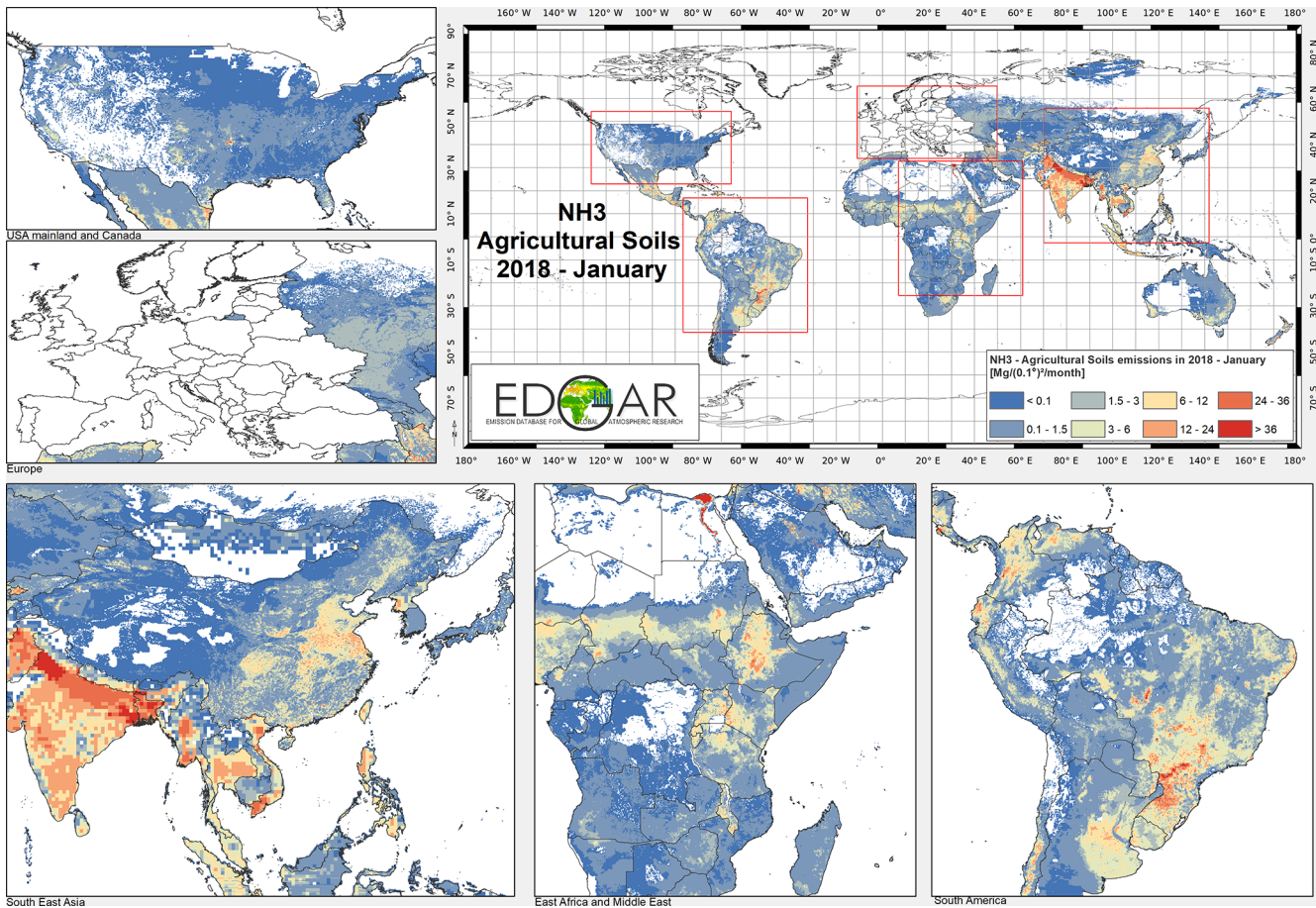


Figure 9. HTAP_v3.2 mosaic: NH_3 emissions from agricultural soil activities in January 2018.

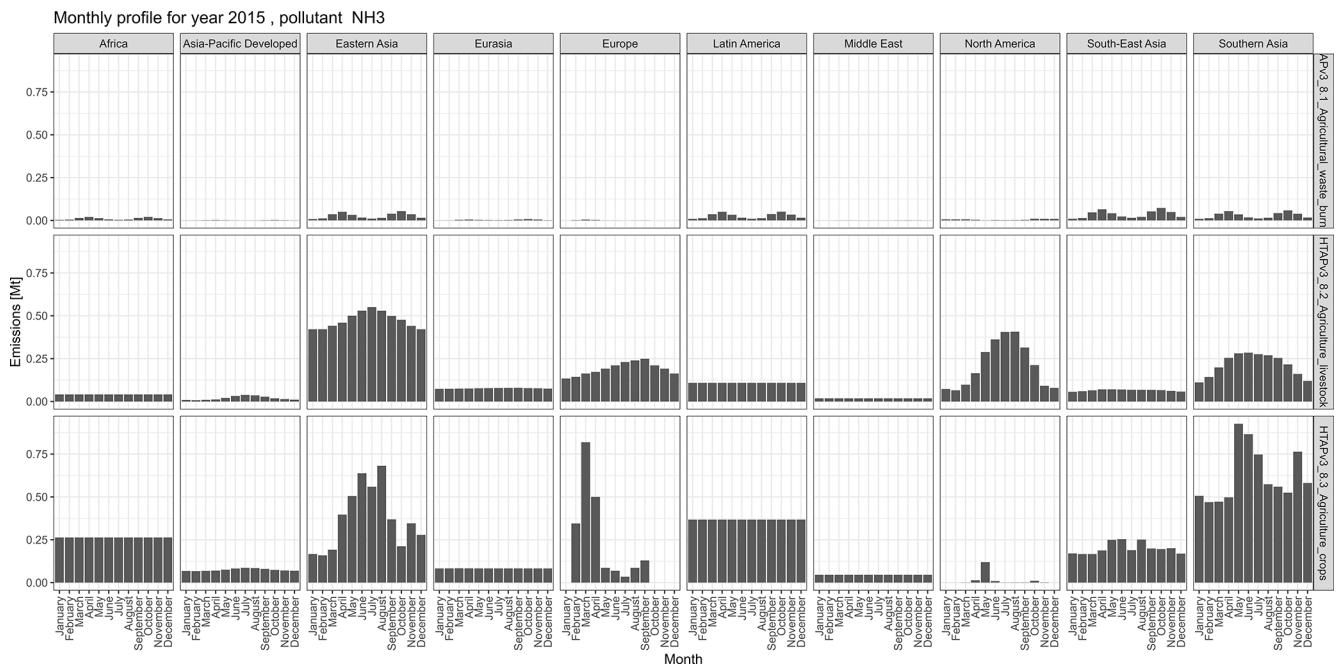


Figure 10. Monthly variability of NH_3 emissions for agriculture-related activities for the different world regions in 2015.

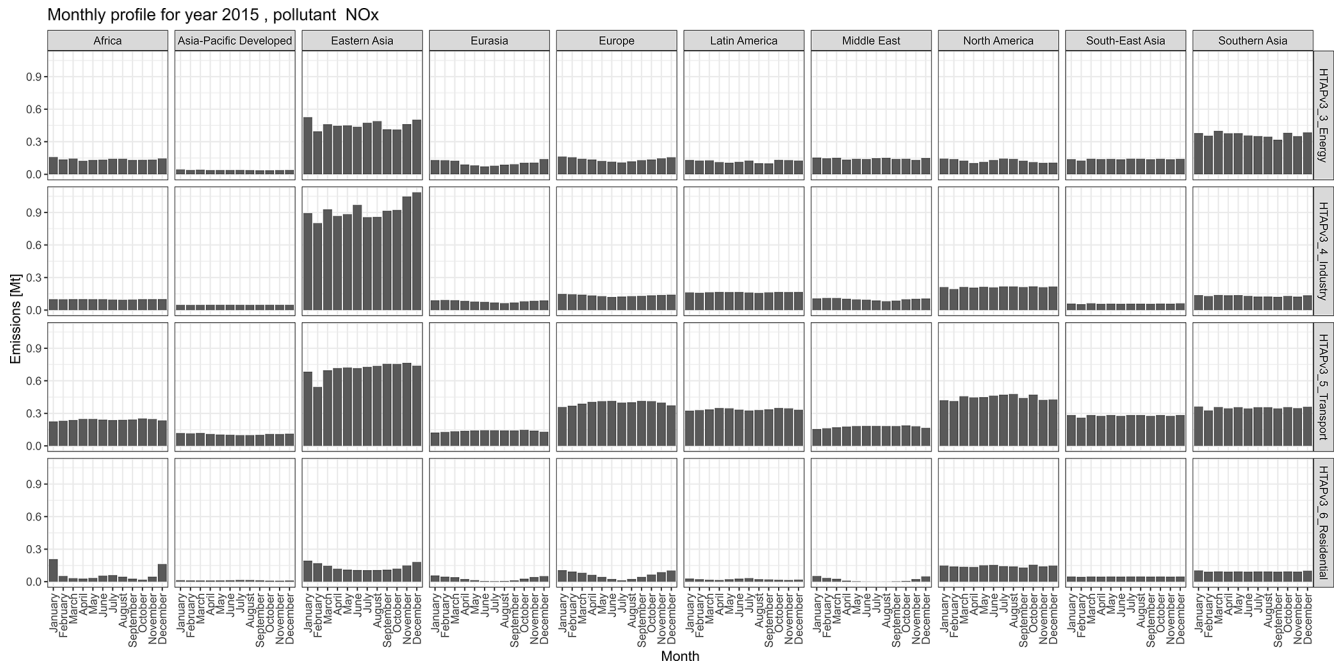


Figure 11. Monthly variability of NO_x emissions for relevant emission sectors for the different world regions in 2015.

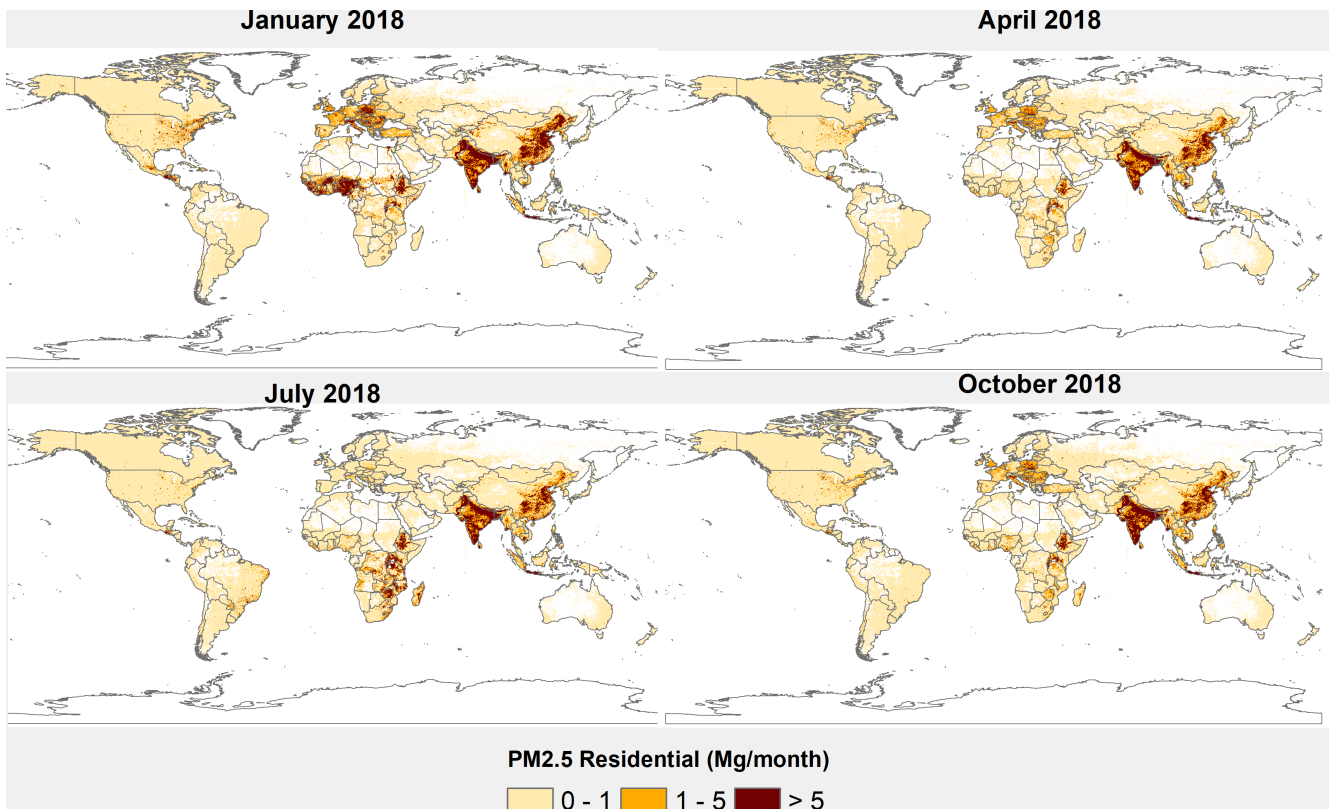


Figure 12. PM_{2.5} monthly emission maps from the residential sector in 2018 from HTAP_v3.2.

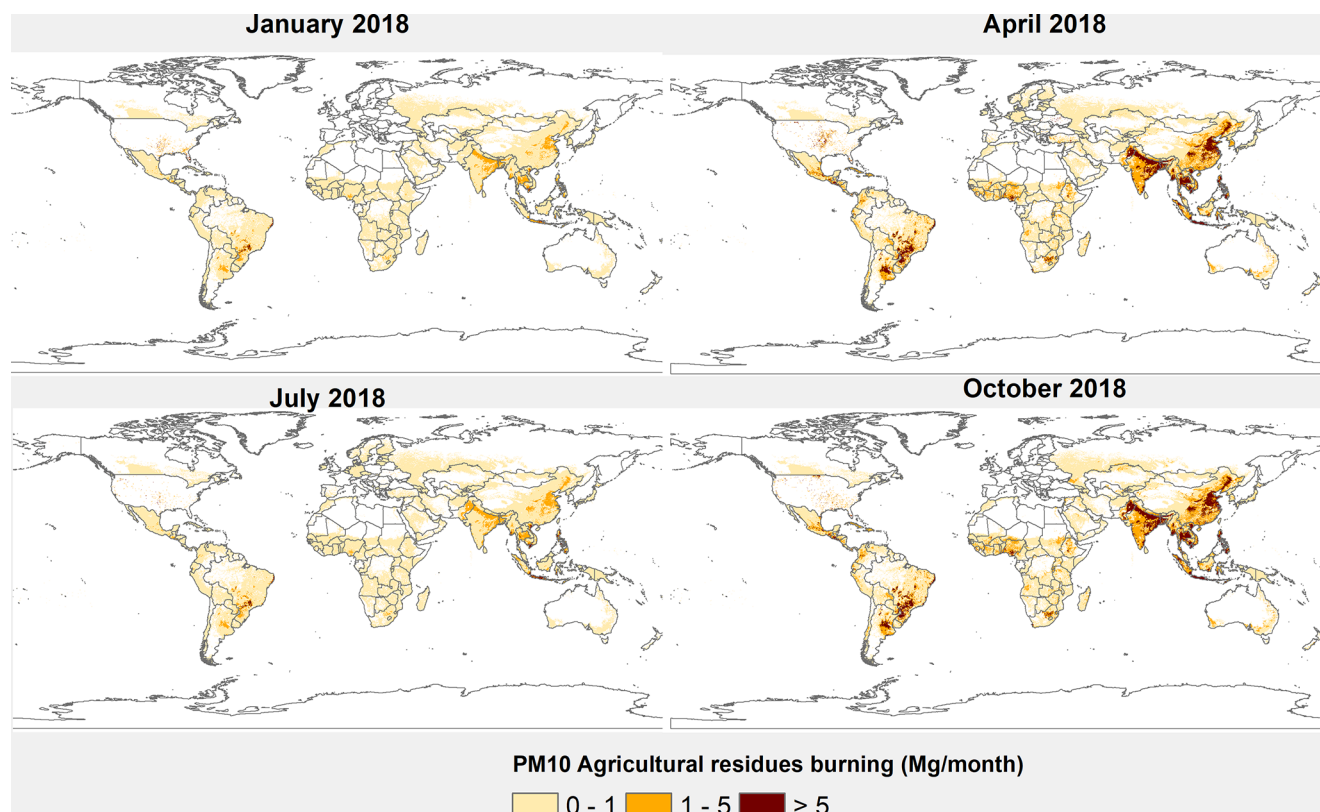


Figure 13. PM₁₀ monthly emission maps from agricultural residue burning in 2018 from HTAP_v3.2.

defined by Huang et al. (2017): Asia; Europe; North America; and Other. The resulting NMVOC speciation is provided as supplementary information to this paper for the 25 NMVOC species (Table S3), 4 world regions, and 15 emitting NMVOC sectors² following the HTAP_v3.2 sector classification (including 13 sectors defined over the 4 world regions, and the two international sectors: international shipping and international aviation). The list of countries comprising each region is also provided in the supplement (Table S4). NMVOC speciation profiles can be accessed at: https://edgar.jrc.ec.europa.eu/dataset_htap_v31#p3 (last access: 27 October 2025).

3.5 Emission Uncertainties

3.5.1 Overview on uncertainties

Unlike greenhouse gas inventories, uncertainty is not routinely estimated for air pollutant emissions by country inventory systems. In part this is due to the different and often disparate processes used to generate air pollution data at the country level (Smith et al., 2022), making it more difficult to conduct uncertainty analysis. While combinations of observational and modelling techniques can be used to evaluate air

²No speciation profile is provided for the “tyre and brake wear sector” not being a source of NMVOC emissions.

pollutant emissions, these are inherently site specific and can be difficult to generalize.

The potential level of uncertainty in any emission estimate depends on how much emission factors vary for a particular activity. We note that the emission species with the lowest uncertainty is carbon dioxide from fossil fuel combustion. This is because CO₂ emission factors are closely tied to fuel energy content, which is a quantity that is tracked and reported by both government and commercial reporting systems. Similar considerations apply to SO₂ emissions, where emissions can be reliably estimated if the sulphur content of fuels and the operational characteristics of emission control devices are known. A key aspect here is that uncertainty in fuel sulphur content is largely uncorrelated across regions, which means that global uncertainty is relatively low, while regional uncertainty often much higher (Smith et al., 2011). On the opposite end of the spectrum, the emission rates for particulate matter depend sensitively on combustion conditions and the operation of any emission control devices and can vary over several orders of magnitude. While this is not an indication of the uncertainty in inventory estimates, this indicates the difficulty of constructing quantitative uncertainty estimates. The type of emission process also influences uncertainty, with fugitive emissions and emissions associated with biological processes generally having higher uncertainty levels.

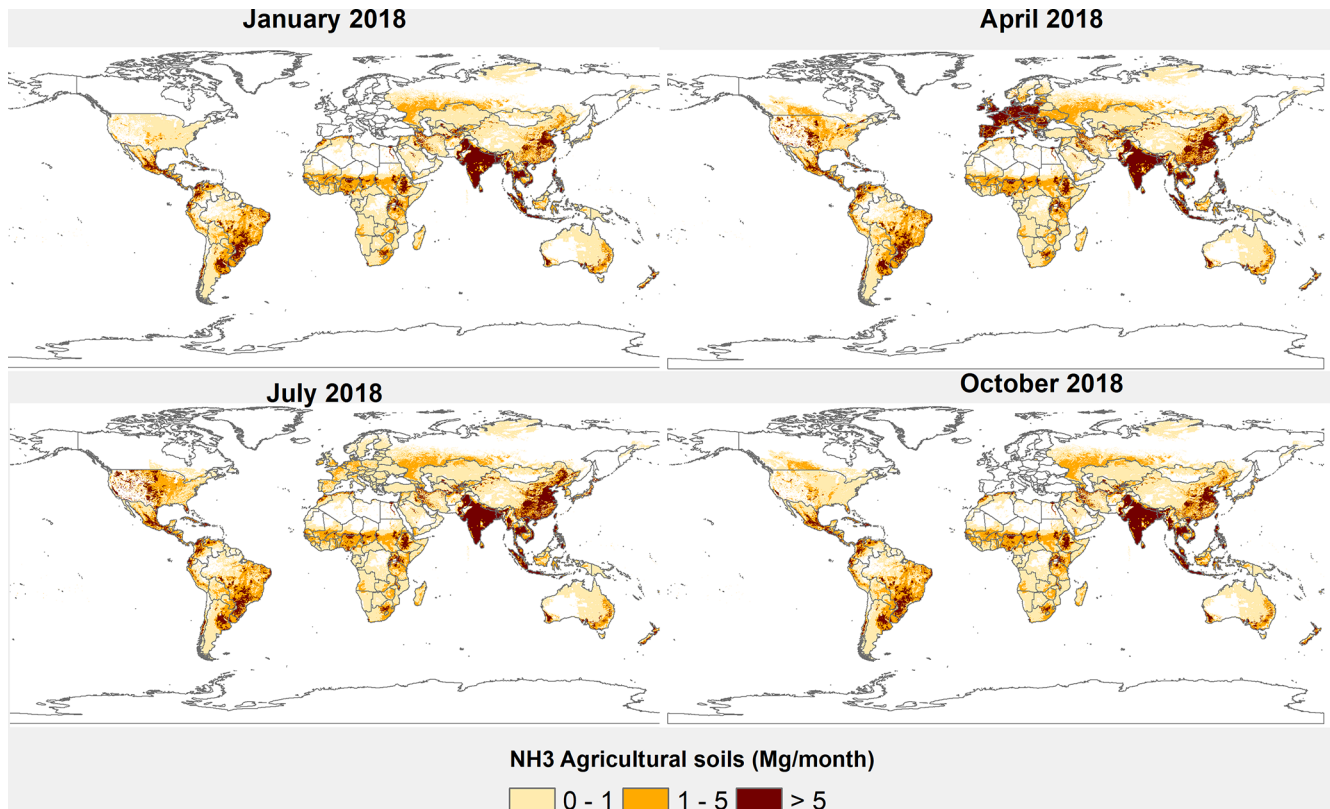


Figure 14. NH₃ monthly emission maps from agricultural soils in 2018 from HTAP_v3.2.

We note also that uncertainty in the overall magnitude of emissions does not necessarily imply a similar level of uncertainty in relative emission trends. Even with uncertainties, the widespread use of emission control devices has resulted in reductions in air pollutant emissions in North America and Europe (Liu et al., 2018; Jamali et al., 2020), as verified by observational and modelling studies.

The emissions in the HTAP_v3.2 mosaic emissions originate from a variety of sources which has some implications for relative uncertainty. Emissions for some regions, such as North America and Europe, were generated by country inventory systems which have been developed and refined over the last several decades. It is reasonable to assume these emissions are robust, however even in these regions detailed studies have indicated that actual emissions in some cases appear to be lower than inventory values (Anderson et al., 2014; Hassler et al., 2016; Travis et al., 2016). Where EDGAR emission estimates were used in the mosaic uncertainties are likely be higher overall given that inventory information developed in those countries was not available for these regions (Solazzo et al., 2021).

Some information on the robustness of the HTAP_v3.2 mosaic can be gained by comparing different inventory estimates, which is shown in Sect. S2. In many cases, the agreement between estimates (for example in North America and Europe) simply indicates common data sources and assump-

tions, although this does indicate that the different inventory groups did conclude that these values were plausible. The larger differences in other regions, however, does point to larger uncertainty there.

3.5.2 Qualitative assessment of the uncertainty of a global emission mosaic

Assessing the uncertainty of a global emission mosaic is challenging since it consists of several bottom-up inventories and by definition it prevents a consistent global uncertainty calculation. Each emission inventory feeding the HTAP_v3.2 mosaic is characterized by its own uncertainty which is documented, where available, by the corresponding literature describing each dataset (see Table 2 and Sect. 2.3). However, the mosaic compilation process may also introduce additional uncertainties compared to the input datasets. In order to limit these additional uncertainties, we made the following considerations:

- for each emission inventory both the national totals and gridded data by sector were gathered. This process allows the mosaic compilers not to introduce additional uncertainty compared to the original input regional datasets. While additional uncertainties may arise from the extraction of the national totals from spatially distributed data (e.g. country border issues which were one

limitation of previous editions of the HTAP mosaics), this is not the case in the current dataset. Therefore, when regional trends are described by region and pollutant (see Sect. 3), no additional source of uncertainty has to be considered from the mosaic compilation approach.

- the sector definition and mapping has been developed following the IPCC categories and when no data was available for a certain combination of sector and pollutant a gapfilling procedure is applied using the EDGAR database. Therefore, the datasets are comparable in terms of sectoral coverage, which reduces uncertainties in this aspect.
- since each inventory provided monthly resolution emission gridmaps and time series there is no additional uncertainty introduced by temporal disaggregation as part of the construction of the HTAP_v3.2 mosaic.

In this work we also provide a qualitative indication of the emission variability by HTAP sector and pollutant at the global level. Table S5 summarises the variability of global HTAP_v3.2 emissions by sector for the boundary years of this mosaic (years 2000, 2018, and 2020) compared to the global EDGARv8.1 data. EDGAR emissions are considered as the reference global emission inventory against which comparing the HTAP_v3.2 estimates although these two global products are not fully independent. The variability of the global emissions is calculated as the relative difference of the estimates of the two inventories, i.e. $(\text{EDGARv8.1-HTAP}_v3.2)/\text{HTAP}_v3.2$. Emission variabilities are also classified as low (L , $L < 15\%$), low medium (LM, $15\% < LM < 50\%$), upper medium (UM, $50\% < UM < 100\%$), high (H , $H > 100\%$), based on the EMEP/EEA Guidebook (2019) information. The largest variability is found in domestic shipping emissions (CO and NMVOC), energy (OC, BC), agricultural crops (PM), road transport (PM, NMVOC) and industry (NH₃, NMVOC). In absence of a full uncertainty assessment the variability can be used as proxy of structural uncertainty, keeping in mind that variability could be biased towards overconfidence, thus underestimating the uncertainty. Moreover, high variability values may be associated to very low emission levels, as in the case of BC and OC emissions from the energy sector as shown in Fig. 2, which will finally not significantly affect the accuracy of total emission estimates. Furthermore, the uncertainty of the spatial proxies has not been assessed and maybe subject of future activity updates.

4 Data availability

The HTAP_v3.2 emission mosaic data can be freely accessed and cited using <https://doi.org/10.5281/zenodo.17086684> (Crippa, 2025). All data can be also accessed through the

EDGAR website at the following link: https://edgar.jrc.ec.europa.eu/dataset_htap_v32 (last access: 27 October 2025).

Data are made available in the following formats:

- Monthly gridmaps of emissions (in Mg month⁻¹) at $0.1 \times 0.1^\circ$ resolution: there is one .NetCDF file per year and substance that includes the emissions for each sector for the 12 months.
- Monthly gridmaps of emission fluxes (in kg m⁻² s⁻¹) at $0.1 \times 0.1^\circ$ resolution: there is one .NetCDF file per year and substance that includes the emission fluxes for each sector the emission fluxes for the 12 months.
- Annual gridmaps of emissions (in Mgyr⁻¹) at $0.1 \times 0.1^\circ$ resolution: there is one .NetCDF file per year and substance that includes the emissions for each sector.
- Annual gridmaps of emission fluxes (in kg m⁻² s⁻¹) at $0.1 \times 0.1^\circ$ resolution: there is one .NetCDF file per year and substance that includes the emission fluxes for each sector.

The full set of HTAP_v3.2 data is quite large, requiring substantial network bandwidth and time for download, and substantial storage space. To make it easier for users to query and use the data, additional products are available. For global modellers who may not require such high spatial resolution, gridmaps at $0.5 \times 0.5^\circ$ resolution are made available following the abovementioned specifications of the higher spatial resolution data. Furthermore, to allow regional modellers to download only the data for the regions they need, the JRC EDGAR group has also developed an interface to allow the users of the HTAP_v3.2 mosaic to extract emission data over arbitrarily specified geographical domains. The HTAP tool is accessible after creation of an ECAS account (<https://webgate.ec.europa.eu/cas/login>, last access: 27 October 2025) and it is available at: https://edgar.jrc.ec.europa.eu/htap_tool/, last access: 27 October 2025.

5 Conclusions

The global air pollution mosaic inventory HTAP_v3.2 presented and discussed in this paper is a state-of-the-art database for addressing the present status and the recent evolution of a set of policy-relevant air pollutants. The inventory is made by the harmonization and blending of seven regional inventories, gapfilled using the most recent release of EDGAR (EDGARv8.1). Compared with the previous version of this dataset (HTAP_v3), the HTAP_v3.2 dataset includes updates to many of the constituent inventories, an extension of the timeseries by two years, and the inclusion of the MEIC emissions for China. By directly incorporating the best available local information, including the spatial distribution of emissions, the HTAP_v3.2 mosaic inventory can be

used for policy-relevant studies at both regional and global levels. As such, the HTAP_v3.2 mosaic inventory provides a complement to globally consistent emission inventories such as EDGAR. The global and regional trends of air pollutant emissions in the HTAP_v3.2 mosaic are comparable with other commonly available global emission datasets.

By providing consistent time series for two decades, HTAP_v3.2 allows an evaluation of the impact and success of the pollution control measures deployed across various regions of the world since 2000. Similarly, its finer sectoral resolution is suitable for understanding how and where technological changes have resulted in emissions reductions, suggesting possible pathways for strengthening appropriate policy actions.

All these features make HTAP_v3.2 a database of interest for policy makers active in the air quality regulatory efforts. HTAP_v3.2 provides a picture of a world where most pollutant emissions are following a steady or decreasing path. However, several areas of the world show an increasing emission trend, with wide portions of the world remaining subjected to unsatisfactory levels of ambient air quality.

When using the HTAP_v3.2 emission mosaic, users should consider the following limitations, for example when combining the HTAP_v3.2 data with other emission input needed to run atmospheric models:

- agricultural waste burning emissions should be treated with caution to avoid double-counting when combined with existing biomass burning emission inventories;
- NMVOC and NO_x emissions from agricultural soils should be treated with caution to avoid double-counting when combining the HTAP_v3.2 data with a natural emissions model such as MEGAN (Model of Emissions of Gases and Aerosols from Nature);
- the speciation of NO_x emissions into its components (NO , NO_2 , HONO) is not provided by the global HTAP_v3.2 mosaic and it is beyond the scope of the current work since the regional inventories report total NO_x with no speciation. Standard practice in global models is to emit all anthropogenic NO_x as NO , while we expect that regional modelling groups will have access to appropriate best practices for their particular regions. In particular for road transport, the partitioning of NO_x emissions between NO , NO_2 , and HONO is highly region-dependent, and it is based on the fleet composition (e.g., number of diesel vehicles relative to gasoline vehicles) and technology level (e.g., the level of exhaust after treatment).

Thanks to the continuous improvement of local and regional emission inventories, recent literature shows new datasets that report regional information over areas of the world not covered by local inventories in the current HTAP_v3.2 mosaic (e.g. Argentina (Puliafito et al. 2021) and

Africa (Keita et al., 2021)). Future updates to this mosaic may also integrate reliable and up to date information over South America or Africa as time and resources permit.

Similar to its predecessors, we expect that this new HTAP_v3.2 mosaic inventory will be used as a basis for global assessments of long-range, transboundary transport of air pollution under the Task Force on Hemispheric Transport of Air Pollution, while also providing a convenient and useful information for regional modellers seeking the best available regional emissions with a consistent gap-filling methodology.

Note on former version. A former version of this article was published on 29 June 2023 and is available at <https://doi.org/10.5194/essd-15-2667-2023>.

Supplement. The supplement related to this article is available online at <https://doi.org/10.5194/essd-17-5915-2025-supplement>.

Author contributions. MC and DG developed the mosaic gathering input from all data providers. The co-chairs of the TF-HTAP (TK, TB, RW and JaKa) fostered the dialogue with international institutions contributing to this work with their data. PM, RM, JR, JZ, DN, MS, MDM, RW provided data for Canada, SC, TM provided data for Japan, JeKu provided data for Europe, J-HW, JiKi provided data for Korea, TK, GP provided data for USA, JuKu provided data for Asia. The JRC EDGAR group (MC, ES, DG, EP, MM, MB, FP) lead the drafting of the publication with input from colleagues contributing to the HTAP_v3.2 mosaic. SJS and HR performed detailed data comparison among available emission inventories. TA calculated and provided the NMVOC speciation fractions for all the sectors for the four regions.

Competing interests. The contact author has declared that none of the authors has any competing interests.

Disclaimer. The views expressed in this article are those of the authors and do not necessarily represent the views or policies of the U.S. Environmental Protection Agency and European Commission. It has been subjected to the Agency's review and has been approved for publication. Note that approval does not signify that the contents necessarily reflect the views of the Agency.

Publisher's note: Copernicus Publications remains neutral with regard to jurisdictional claims made in the text, published maps, institutional affiliations, or any other geographical representation in this paper. While Copernicus Publications makes every effort to include appropriate place names, the final responsibility lies with the authors. Views expressed in the text are those of the authors and do not necessarily reflect the views of the publisher.

Acknowledgements. The authors would like to thank all HTAP_v3.2 data providers for the fruitful cooperation.

No external funding was used for this research.

Financial support. J-STREAM emission inventory for Japan was developed by Environment Research and Technology Development Fund (grant nos. JPMEERF20165001 and JPMEERF20215005) of the Environmental Restoration and Conservation Agency Provided by the Ministry of Environment of Japan, and FRIEND (Fine Particle Research Initiative in East Asia Considering National Differences) Project through the National Research Foundation of Korea (NRF) funded by the Ministry of Science and ICT (grant no. 2020M3G1A1114622). REASv3.2.1 has been supported by the Environmental Research and Technology Development Fund (grant no. S-12 and S-20 (JPMEERF21S12012)) of the Environmental Restoration and Conservation Agency of Japan and the Japan Society for the Promotion of Science, KAKENHI (grant no. 19K12303).

Review statement. This paper was edited by Yuqiang Zhang and reviewed by two anonymous referees.

References

- Álamos, N., Huneus, N., Opazo, M., Osses, M., Puja, S., Pan-toja, N., Denier van der Gon, H., Schueftan, A., Reyes, R., and Calvo, R.: High-resolution inventory of atmospheric emissions from transport, industrial, energy, mining and residential activities in Chile, *Earth Syst. Sci. Data*, 14, 361–379, <https://doi.org/10.5194/essd-14-361-2022>, 2022.
- Anderson, D. C., Loughner, C. P., Diskin, G., Weinheimer, A., Canty, T. P., Salawitch, R. J., Worden, H. M., Fried, A., Mikoviny, T., Wisthaler, A., and Dickerson, R. R.: Measured and modeled CO and NO_y in DISCOVER-AQ: An evaluation of emissions and chemistry over the eastern US, *Atmospheric Environment*, 96, 78–87, <https://doi.org/10.1016/j.atmosenv.2014.07.004>, 2014.
- APEI: Air Pollutant Emissions Inventory: overview, Canada.ca, <https://www.canada.ca/content/dam/eccc/images/apei/apei-2018-en.pdf> (last access: 27 October 2025), 2018.
- APEI: Canada's Air Pollutant Emissions Inventory Report 1990–2019, Environment and Climate Change Canada, Gatineau, Quebec, 99 pp., https://publications.gc.ca/collections/collection_2021/eccc/En81-30-2019-eng.pdf (last access: 27 October 2025), 2021.
- NIES, Center for Global Environmental Research, Earth System Division, and National Institute for Environmental Studies: National Greenhouse Gas Inventory Report of JAPAN 2022, Greenhouse Gas Inventory Office of Japan and Ministry of the Environment, Japan, <https://www.nies.go.jp/gio/en/> (last access: 27 October 2025), 2022.
- Chatani, S., Shimadera, H., Itahashi, S., and Yamaji, K.: Comprehensive analyses of source sensitivities and apportionments of PM_{2.5} and ozone over Japan via multiple numerical techniques, *Atmos. Chem. Phys.*, 20, 10311–10329, <https://doi.org/10.5194/acp-20-10311-2020>, 2020.
- Chatani, S., Yamaji, K., Sakurai, T., Itahashi, S., Shimadera, H., Kitayama, K., and Hayami, H. J. A.: Overview of model inter-comparison in Japan's study for reference air quality modeling (J-STREAM), *Atmosphere*, 9, 19, <https://doi.org/10.3390/atmos9010019>, 2018.
- Chatani, S., Kitayama, K., Itahashi, S., Irie, H., and Shimadera, H.: Effectiveness of emission controls implemented since 2000 on ambient ozone concentrations in multiple timescales in Japan: An emission inventory development and simulation study, *Science of The Total Environment*, 894, 165058, <https://doi.org/10.1016/j.scitotenv.2023.165058>, 2023.
- Chutia, L., Wang, J., Zhang, H., Chen, X., Castro Garcia, L., and Janecek, N.: Elucidating the impacts of aerosol radiative effects for mitigating surface O₃ and PM_{2.5} in Delhi, India during crop residue burning period, *Atmospheric Environment*, 339, 120890, <https://doi.org/10.1016/j.atmosenv.2024.120890>, 2024.
- Clayton, C. J., Marsh, D. R., Turnock, S. T., Graham, A. M., Pringle, K. J., Reddington, C. L., Kumar, R., and McQuaid, J. B.: The co-benefits of a low-carbon future for PM_{2.5} and O₃ air pollution in Europe, *Atmos. Chem. Phys.*, 24, 10717–10740, <https://doi.org/10.5194/acp-24-10717-2024>, 2024.
- Copernicus Land Monitoring Service: CORINE Land Cover 2012, <https://land.copernicus.eu/pan-european/corine-land-cover/clc-2012> (last access: 13 August 2018), 2016.
- Crippa, M.: HTAP_v3.2 emission mosaic, Zenodo [data set], <https://doi.org/10.5281/zenodo.17086684>, 2025.
- Crippa, M., Janssens-Maenhout, G., Dentener, F., Guizzardi, D., Sindelarova, K., Muntean, M., Van Dingenen, R., and Granier, C.: Forty years of improvements in European air quality: regional policy-industry interactions with global impacts, *Atmos. Chem. Phys.*, 16, 3825–3841, <https://doi.org/10.5194/acp-16-3825-2016>, 2016.
- Crippa, M., Guizzardi, D., Muntean, M., Schaaf, E., Dentener, F., van Aardenne, J. A., Monni, S., Doering, U., Olivier, J. G. J., Pagliari, V., and Janssens-Maenhout, G.: Gridded emissions of air pollutants for the period 1970–2012 within EDGAR v4.3.2, *Earth Syst. Sci. Data*, 10, 1987–2013, <https://doi.org/10.5194/essd-10-1987-2018>, 2018.
- Crippa, M., Solazzo, E., Huang, G., Guizzardi, D., Koffi, E., Muntean, M., Schieberle, C., Friedrich, R., and Janssens-Maenhout, G.: High resolution temporal profiles in the Emissions Database for Global Atmospheric Research, *Scientific Data*, 7, 121, <https://doi.org/10.1038/s41597-020-0462-2>, 2020.
- Crippa, M., Guizzardi, D., Pisoni, E., Solazzo, E., Guion, A., Muntean, M., Florczyk, A., Schiavina, M., Melchiorri, M., and Hutfilter, A. F.: Global anthropogenic emissions in urban areas: patterns, trends, and challenges, *Environmental Research Letters*, 16, 074033, <https://doi.org/10.1088/1748-9326/ac00e2>, 2021a.
- Crippa, M., Guizzardi, D., Solazzo, E., Muntean, M., Schaaf, E., Monforti-Ferrario, F., Banja, M., Olivier, J. G. J., Grassi, G., Rossi, S., and Vignati, E.: GHG emissions of all world countries – 2021 Report, EUR 30831 EN, Publications Office of the European Union, Luxembourg, ISBN 978-92-76-41547-3, <https://doi.org/10.2760/173513>, 2021b.
- Crippa, M., Guizzardi, D., Butler, T., Keating, T., Wu, R., Kaminski, J., Kuenen, J., Kurokawa, J., Chatani, S., Morikawa, T., Pouliot, G., Racine, J., Moran, M. D., Klimont, Z., Manseau, P. M., Mashayekhi, R., Henderson, B. H., Smith, S. J., Suchyta, H., Muntean, M., Solazzo, E., Banja, M., Schaaf, E., Pagani, F., Woo,

- J.-H., Kim, J., Monforti-Ferrario, F., Pisoni, E., Zhang, J., Niemi, D., Sassi, M., Ansari, T., and Foley, K.: The HTAP_v3 emission mosaic: merging regional and global monthly emissions (2000–2018) to support air quality modelling and policies, *Earth Syst. Sci. Data*, 15, 2667–2694, <https://doi.org/10.5194/essd-15-2667-2023>, 2023.
- Crippa, M., Guizzardi, D., Pagani, F., Schiavina, M., Melchiorri, M., Pisoni, E., Graziosi, F., Muntean, M., Maes, J., Dijkstra, L., Van Damme, M., Clarisse, L., and Coheur, P.: Insights into the spatial distribution of global, national, and subnational greenhouse gas emissions in the Emissions Database for Global Atmospheric Research (EDGAR v8.0), *Earth Syst. Sci. Data*, 16, 2811–2830, <https://doi.org/10.5194/essd-16-2811-2024>, 2024.
- Diamond, M. S.: Detection of large-scale cloud microphysical changes within a major shipping corridor after implementation of the International Maritime Organization 2020 fuel sulfur regulations, *Atmos. Chem. Phys.*, 23, 8259–8269, <https://doi.org/10.5194/acp-23-8259-2023>, 2023.
- Denier van der Gon, H. A. C., Bergström, R., Fountoukis, C., Johansson, C., Pandis, S. N., Simpson, D., and Visschedijk, A. J. H.: Particulate emissions from residential wood combustion in Europe – revised estimates and an evaluation, *Atmos. Chem. Phys.*, 15, 6503–6519, <https://doi.org/10.5194/acp-15-6503-2015>, 2015.
- Ding, J., van der A, R., Eskes, H., Dammers, E., Shephard, M., Wichink Kruit, R., Guevara, M., and Tarrason, L.: Ammonia emission estimates using CrIS satellite observations over Europe, *Atmos. Chem. Phys.*, 24, 10583–10599, <https://doi.org/10.5194/acp-24-10583-2024>, 2024.
- EEA: Emission trends of sulphur oxides, https://www.eea.europa.eu/data-and-maps/daviz/emission-trends-of-sulphur-oxides#tab-chart_1 (last access: 22 October 2022), 2022.
- EMEP/EEA: EMEP/EEA Air Pollutant Emission Inventory Guidebook 2013. Technical Guidance to Prepare National Emission Inventories, Luxembourg: Publications Office of the European Union, Technical Report No. 12/2013, <https://www.eea.europa.eu/en/analysis/publications/emep-eea-guidebook-2013> (last access: 27 October 2025), 2013.
- EMEP/EEA: EMEP/EEA air pollutant emission inventory guidebook 2016, EEA Report No. 21/2016, <https://www.eea.europa.eu/en/analysis/publications/emep-eea-guidebook-2016> (last access: 27 October 2025), 2016.
- EMEP/EEA: EMEP/EEA air pollutant emission inventory guidebook 2019, European Environment Agency, 2019, Luxembourg, Publications Office of the European Union, ISBN 978-92-9480-098-5, <https://doi.org/10.2800/293657>, 2019.
- European Commission: Directive 2001/80/EC of the European Parliament and of the Council of 23 October 2001 on the limitation of emissions of certain pollutants into the air from large combustion plants, <https://eur-lex.europa.eu/legal-content/EN/TXT/?uri=celex%3A32001L0080> (last access: 1 July 2021), 2001.
- European Commission: Directive (EU) 2016/2284 on the reduction of national emissions of certain atmospheric pollutants, https://eur-lex.europa.eu/legal-content/EN/TXT/?uri=uriserv:OJ.L_.2016.344.01.0001.01.ENG&toc=OJ:L:2016:344:TOC (last access: 1 July 2021), 2016.
- Faber, J., Hanayama, S., Zhang, S., Pereda, P., Comer, B., Hauerhof, E., van der Loeff, W., Smith, T., Zhang, Y., Kosaka, H., Adachi, M., Bonello, J., Galbraith, C., Gong, Z., Hirata, K., Hummels, D., Kleijn, A., Lee, D., Liu, Y., Lucchesi, A., Mao, X., Muraoka, E., Osipova, L., Qian, H., Rutherford, D., la Fuente, S., Yuan, H., Perico, C., Wu, L., Sun, D., Yoo, D., and Xing, H.: Fourth IMO GHG Study, MEPC 75-7-15, https://greenvoyage2050.imo.org/wp-content/uploads/2021/07/Fourth-IMO-GHG-Study-2020-Full-report-and-annexes_compressed.pdf (last access: 27 October 2025), 2020.
- FAO: Gridded Livestock of the World (GLW3), <http://www.fao.org/land-water/land/land-governance/land-resources-planning-toolbox/category/details/en/c/1236449/> (last access: 10 August 2018), 2010.
- FAOSTAT: Statistics Division of the Food and Agricultural Organisation of the UN, <https://www.fao.org/faostat> (last access: 30 April 2023), 2023.
- Foley, K. M., Pouliot, G. A., Eyth, A., Aldridge, M. F., Allen, C., Appel, K. W., Bash, J. O., Beardsley, M., Beidler, J., Choi, D., Farkas, C., Gilliam, R. C., Godfrey, J., Henderson, B. H., Hogrefe, C., Koplitz, S. N., Mason, R., Mathur, R., Misener, C., Possiel, N., Pye, H. O. T., Reynolds, L., Roark, M., Roberts, S., Schwede, D. B., Seltzer, K. M., Sonntag, D., Talgo, K., Toro, C., Vukovich, J., Xing, J., and Adams, E.: 2002–2017 anthropogenic emissions data for air quality modeling over the United States, *Data in Brief*, 47, 109022, <https://doi.org/10.1016/j.dib.2023.109022>, 2023.
- Geng, G., Liu, Y., Liu, Y., Liu, S., Cheng, J., Yan, L., Wu, N., Hu, H., Tong, D., Zheng, B., Yin, Z., He, K., and Zhang, Q.: Efficacy of China's clean air actions to tackle PM_{2.5} pollution between 2013 and 2020, *Nature Geoscience*, 17, 987–994, <https://doi.org/10.1038/s41561-024-01540-z>, 2024.
- Graham, A. M., Spracklen, D. V., McQuaid, J. B., Smith, T. E. L., Nurrahmawati, H., Ayona, D., Mulawarman, H., Adam, C., Papargyropoulou, E., Rigby, R., Padfield, R., and Choiruzzad, S.: Updated Smoke Exposure Estimate for Indonesian Peatland Fires Using a Network of Low-Cost PM_{2.5} Sensors and a Regional Air Quality Model, *GeoHealth*, 8, e2024GH001125, <https://doi.org/10.1029/2024GH001125>, 2024.
- Guevara, M., Jorba, O., Tena, C., Denier van der Gon, H., Kuenen, J., Elguindi, N., Darras, S., Granier, C., and Pérez García-Pando, C.: Copernicus Atmosphere Monitoring Service TEMPO profiles (CAM5-TEMPO): global and European emission temporal profile maps for atmospheric chemistry modelling, *Earth Syst. Sci. Data*, 13, 367–404, <https://doi.org/10.5194/essd-13-367-2021>, 2021.
- Hassler, B., McDonald, B. C., Frost, G. J., Borbon, A., Carslaw, D. C., Civerolo, K., Granier, C., Monks, P. S., Monks, S., Parrish, D. D., Pollack, I. B., Rosenlof, K. H., Ryerson, T. B., von Schneidemesser, E., and Trainer, M.: Analysis of long-term observations of NO_x and CO in megacities and application to constraining emissions inventories, *Geophysical Research Letters*, 43, 9920–9930, <https://doi.org/10.1002/2016GL069894>, 2016.
- Hu, A.-G.: The Five-Year Plan: A new tool for energy saving and emissions reduction in China, *J. Advances in Climate Change Research*, 7, 222–228, <https://doi.org/10.1016/j.accre.2016.12.005>, 2016.
- Hu, Y., Yu, H., Kang, S., Yang, J., Chen, X., Yin, X., and Chen, P.: Modeling the transport of PM₁₀, PM_{2.5}, and O₃ from South Asia to the Tibetan Plateau, *Atmospheric Research*, 303, 107323, <https://doi.org/10.1016/j.atmosres.2024.107323>, 2024.

- Huang, G., Brook, R., Crippa, M., Janssens-Maenhout, G., Schieberle, C., Dore, C., Guizzardi, D., Muntean, M., Schaaf, E., and Friedrich, R.: Speciation of anthropogenic emissions of non-methane volatile organic compounds: a global gridded data set for 1970–2012, *Atmos. Chem. Phys.*, 17, 7683–7701, <https://doi.org/10.5194/acp-17-7683-2017>, 2017.
- Huang, L., Zhao, B., Wang, S., Chang, X., Klimont, Z., Huang, G., Zheng, H., and Hao, J.: Global Anthropogenic Emissions of Full-Volatility Organic Compounds, *Environ. Sci. Technol.*, 57, 16435–16445, <https://doi.org/10.1021/acs.est.3c04106>, 2023.
- Huneus, N., van Der Gon, H. D., Castesana, P., Menares, C., Granier, C., Granier, L., Alonso, M., de Fatima Andrade, M., Dawidowski, L., and Gallardo, L. J. A. E.: Evaluation of anthropogenic air pollutant emission inventories for South America at national and city scale, *Atmospheric Environment*, 235, 117606, <https://doi.org/10.1016/j.atmosenv.2020.117606>, 2020.
- ICAO: International Civil Aviation Organisation data: Airline Route Mapper data, <http://arm.64hosts.com/> (last access: 27 October 2025), 2015.
- IEA: World Energy Balances 2022 Edition, <https://www.iea.org/data-and-statistics> (last access: 27 October 2025), 2022.
- IIASA: Progress towards the achievement of the EU's Air Quality and Emission Objectives, https://ec.europa.eu/environment/air/pdf/clean_air_outlook_overview_report.pdf (last access: 1 July 2021) 2018.
- IMO: Third IMO GHG Study 2014, MEPC-67-6-INF3-2014, <https://www.imo.org/en/ourwork/environment/pages/greenhouse-gas-studies-2014.aspx> (last access: 27 October 2025), 2014.
- IMO: Fourth IMO GHG Study 2020, MEPC 75-7-15, <https://www.imo.org/en/ourwork/environment/pages/fourth-imo-greenhouse-gas-study-2020.aspx> (last access: 27 October 2025), 2020.
- IPCC: Revised 1996 IPCC Guidelines for National Greenhouse Gas Inventories: Reporting Instructions, <https://www.ipcc-nggip.iges.or.jp/public/gl/guidelin/ch1ri.pdf> (last access: 27 October 2025), 1996.
- IPCC: Guidelines for National Greenhouse Gas Inventory, Volume 5: Waste. Internet, <http://www.ipcc-nggip.iges.or.jp/public/2006gl/vol5.html> (last access: 27 October 2025), 2006.
- Itahashi, S.: Severe level of photochemical oxidants (O_x) over the western coast of Japan during autumn after typhoon passing, *Sci. Rep.*, 13, 16369, <https://doi.org/10.1038/s41598-023-43485-0>, 2023.
- Itahashi, S., Terao, Y., Ikeda, K., and Tanimoto, H.: Source identification of carbon monoxide over the greater Tokyo area: Tower measurement network and evaluation of global/regional model simulations at different resolutions, *Atmospheric Environment: X*, 23, 100284, <https://doi.org/10.1016/j.aeoa.2024.100284>, 2024.
- Jalkanen, J.-P., Johansson, L., Kukkonen, J., Brink, A., Kalli, J., and Stipa, T.: Extension of an assessment model of ship traffic exhaust emissions for particulate matter and carbon monoxide, *Atmos. Chem. Phys.*, 12, 2641–2659, <https://doi.org/10.5194/acp-12-2641-2012>, 2012.
- Jamali, S., Klingmyr, D., and Tagesson, T.: Global-Scale Patterns and Trends in Tropospheric NO_2 Concentrations, 2005–2018, *Remote Sensing*, 12, 3526, <https://doi.org/10.3390/rs12213526>, 2020.
- Janssens-Maenhout, G., Dentener, F., Van Aardenne, J., Monni, S., Pagliari, V., Orlandini, L., Klimont, Z., Kurokawa, J.-i., Akimoto, H., and Ohara, T.: EDGAR-HTAP: a harmonized gridded air pollution emission dataset based on national inventories, European Commission Publications Office, Ispra, Italy, <https://doi.org/10.2788/14069>, 2012.
- Janssens-Maenhout, G., Crippa, M., Guizzardi, D., Dentener, F., Muntean, M., Pouliot, G., Keating, T., Zhang, Q., Kurokawa, J., Wankmüller, R., Denier van der Gon, H., Kuenen, J. J. P., Klimont, Z., Frost, G., Darras, S., Koffi, B., and Li, M.: HTAP_v2.2: a mosaic of regional and global emission grid maps for 2008 and 2010 to study hemispheric transport of air pollution, *Atmos. Chem. Phys.*, 15, 11411–11432, <https://doi.org/10.5194/acp-15-11411-2015>, 2015.
- Janssens-Maenhout, G., Crippa, M., Guizzardi, D., Muntean, M., Schaaf, E., Dentener, F., Bergamaschi, P., Pagliari, V., Olivier, J. G. J., Peters, J. A. H. W., van Aardenne, J. A., Monni, S., Doering, U., Petrescu, A. M. R., Solazzo, E., and Oreggioni, G. D.: EDGAR v4.3.2 Global Atlas of the three major greenhouse gas emissions for the period 1970–2012, *Earth Syst. Sci. Data*, 11, 959–1002, <https://doi.org/10.5194/essd-11-959-2019>, 2019.
- Johansson, L., Jalkanen, J.-P., and Kukkonen, J.: Global assessment of shipping emissions in 2015 on a high spatial and temporal resolution, *Atmospheric Environment*, 167, 403–415, <https://doi.org/10.1016/j.atmosenv.2017.08.042>, 2017.
- Kaiser, J. W., Heil, A., Andreae, M. O., Benedetti, A., Chubarova, N., Jones, L., Morcrette, J.-J., Razinger, M., Schultz, M. G., Suttie, M., and van der Werf, G. R.: Biomass burning emissions estimated with a global fire assimilation system based on observed fire radiative power, *Biogeosciences*, 9, 527–554, <https://doi.org/10.5194/bg-9-527-2012>, 2012.
- Keita, S., Lioussé, C., Assamoi, E.-M., Doumbia, T., N'Datchoh, E. T., Gnamien, S., Elguindi, N., Granier, C., and Yoboué, V.: African anthropogenic emissions inventory for gases and particles from 1990 to 2015, *Earth Syst. Sci. Data*, 13, 3691–3705, <https://doi.org/10.5194/essd-13-3691-2021>, 2021.
- Kim, J., Park, J., Hu, H., Crippa, M., Guizzardi, D., Chatani, S., Kurokawa, J., Morikawa, T., Yeo, S., Jin, H., and Woo, J.-H.: Long-term historical trends in air pollutant emissions in South Korea (2000–2018), *Asian J. Atmos. Environ.*, 17, 12, <https://doi.org/10.1007/s44273-023-00013-w>, 2023a.
- Kim, K.-M., Kim, S.-W., Seo, S., Blake, D. R., Cho, S., Crawford, J. H., Emmons, L. K., Fried, A., Herman, J. R., Hong, J., Jung, J., Pfister, G. G., Weinheimer, A. J., Woo, J.-H., and Zhang, Q.: Sensitivity of the WRF-Chem v4.4 simulations of ozone and formaldehyde and their precursors to multiple bottom-up emission inventories over East Asia during the KORUS-AQ 2016 field campaign, *Geosci. Model Dev.*, 17, 1931–1955, <https://doi.org/10.5194/gmd-17-1931-2024>, 2024.
- Kim, S.-W., Kim, K.-M., Jeong, Y., Seo, S., Park, Y., and Kim, J.: Changes in surface ozone in South Korea on diurnal to decadal timescales for the period of 2001–2021, *Atmos. Chem. Phys.*, 23, 12867–12886, <https://doi.org/10.5194/acp-23-12867-2023>, 2023b.
- Kong, L., Tang, X., Wang, Z., Zhu, J., Li, J., Wu, H., Wu, Q., Chen, H., Zhu, L., Wang, W., Liu, B., Wang, Q., Chen, D., Pan, Y., Li, J., Wu, L., and Carmichael, G. R.: Changes in air pollutant emissions in China during two clean-air action periods derived from the newly developed Inversed Emission Inventory for Chinese

- Air Quality (CAQIEI), *Earth Syst. Sci. Data*, 16, 4351–4387, <https://doi.org/10.5194/essd-16-4351-2024>, 2024.
- Kuener, J., Dellaert, S., Visschedijk, A., Jalkanen, J.-P., Supper, I., and Denier van der Gon, H.: CAMS-REG-v4: a state-of-the-art high-resolution European emission inventory for air quality modelling, *Earth Syst. Sci. Data*, 14, 491–515, <https://doi.org/10.5194/essd-14-491-2022>, 2022.
- Kurokawa, J. and Ohara, T.: Long-term historical trends in air pollutant emissions in Asia: Regional Emission inventory in ASIA (REAS) version 3, *Atmos. Chem. Phys.*, 20, 12761–12793, <https://doi.org/10.5194/acp-20-12761-2020>, 2020.
- Lekaki, D., Kastori, M., Papadimitriou, G., Mellios, G., Guizzardi, D., Muntean, M., Crippa, M., Oreggioni, G., and Ntziachristos, L.: Road transport emissions in EDGAR (Emissions Database for Global Atmospheric Research), *Atmospheric Environment*, <https://doi.org/10.1016/j.atmosenv.2024.120422>, 2024.
- Li, M., Liu, H., Geng, G., Hong, C., Liu, F., Song, Y., Tong, D., Zheng, B., Cui, H., Man, H., Zhang, Q., and He, K.: Anthropogenic emission inventories in China: a review, *Natl. Sci. Rev.*, 4, 834–866, 2017.
- Liu, F., Zhang, Q., Tong, D., Zheng, B., Li, M., Huo, H., and He, K. B.: High-resolution inventory of technologies, activities, and emissions of coal-fired power plants in China from 1990 to 2010, *Atmos. Chem. Phys.*, 15, 13299–13317, <https://doi.org/10.5194/acp-15-13299-2015>, 2015.
- Liu, F., Choi, S., Li, C., Fioletov, V. E., McLinden, C. A., Joiner, J., Krotkov, N. A., Bian, H., Janssens-Maenhout, G., Darmenov, A. S., and da Silva, A. M.: A new global anthropogenic SO₂ emission inventory for the last decade: a mosaic of satellite-derived and bottom-up emissions, *Atmos. Chem. Phys.*, 18, 16571–16586, <https://doi.org/10.5194/acp-18-16571-2018>, 2018.
- Liu, J., Tong, D., Zheng, Y., Cheng, J., Qin, X., Shi, Q., Yan, L., Lei, Y., and Zhang, Q.: Carbon and air pollutant emissions from China's cement industry 1990–2015: trends, evolution of technologies, and drivers, *Atmos. Chem. Phys.*, 21, 1627–1647, <https://doi.org/10.5194/acp-21-1627-2021>, 2021.
- Liu, J., Christensen, J. H., Ye, Z., Dong, S., Geels, C., Brandt, J., Nenes, A., Yuan, Y., and Im, U.: Impact of meteorology and aerosol sources on PM_{2.5} and oxidative potential variability and levels in China, *Atmos. Chem. Phys.*, 24, 10849–10867, <https://doi.org/10.5194/acp-24-10849-2024>, 2024.
- Mao, Y., Wang, H., Jiang, F., Feng, S., Jia, M., and Ju, W.: Anthropogenic NO_x emissions of China, the U.S. and Europe from 2019 to 2022 inferred from TROPOMI observations, *Environ. Res. Lett.*, 19, 054024, <https://doi.org/10.1088/1748-9326/ad3cf9>, 2024.
- Nalam, A., Lupaşcu, A., Ansari, T., and Butler, T.: Regional and sectoral contributions of NO_x and reactive carbon emission sources to global trends in tropospheric ozone during the 2000–2018 period, *Atmos. Chem. Phys.*, 25, 5287–5311, <https://doi.org/10.5194/acp-25-5287-2025>, 2025.
- Nawaz, M. O., Henze, D. K., Huneed, N. J., Osses, M., Álamos, N., Opazo, M. A., and Gallardo, L.: Sources of Air Pollution Health Impacts and Co-Benefits of Carbon Neutrality in Santiago, Chile, *J. Geophys. Res.-Atmos.*, 128, e2023JD038808, <https://doi.org/10.1029/2023JD038808>, 2023.
- NPRI: National Pollutant Release Inventory Summary Report 2016, https://publications.gc.ca/collections/collection_2017 eccc/En81-14-2016-eng.pdf (last access: 27 October 2025), 2017.
- Open Street Map: Open Street Map, <https://www.openstreetmap.org/> (last access: 8 March 2019), 2017.
- OpenTransportMap: Open Transport Map, <http://opentransportmap.info/> (last access: 8 March 2019), 2017.
- Osipova, L., Georgeff, E., and Comer, B.: Global scrubber wastewater discharges under IMO's 2020 fuel sulfur limit, International Council on Clean Transportation, <https://theicct.org/wp-content/uploads/2021/06/scrubber-discharges-Apr2021.pdf> (last access: 27 October 2025), 2021.
- Patel, A., Mallik, C., Chandra, N., Patra, P. K., and Steinbacher, M.: Revisiting regional and seasonal variations in decadal carbon monoxide variability: Global reversal of growth rate, *Science of The Total Environment*, 909, 168476, <https://doi.org/10.1016/j.scitotenv.2023.168476>, 2024.
- Peng, L., Zhang, Q., Yao, Z., Mauzerall, D. L., Kang, S., Du, Z., Zheng, Y., Xue, T., and He, K.: Underreported coal in statistics: A survey-based solid fuel consumption and emission inventory for the rural residential sector in China, *Applied Energy*, 235, 1169–1182, <https://doi.org/10.1016/j.apenergy.2018.11.043>, 2019.
- Planning Commission: Eleventh Five Year Plan 2007-12, Volume-I. Inclusive Growth, http://www.gov.cn/zhengce/content/2008-03/28/content_4877.htm (last access: 27 October 2025), 2008.
- Platts: World Electric Power Plants database, <https://www.spglobal.com/platts/en/commodities/electric-power> (last access: 21 February 2018), 2017.
- Puliafito, S. E., Bolaño-Ortiz, T. R., Fernandez, R. P., Berná, L. L., Pascual-Flores, R. M., Urquiza, J., López-Noreña, A. I., and Tames, M. F.: High-resolution seasonal and decadal inventory of anthropogenic gas-phase and particle emissions for Argentina, *Earth Syst. Sci. Data*, 13, 5027–5069, <https://doi.org/10.5194/essd-13-5027-2021>, 2021.
- Sassi, M., Zhang, J., and Moran, M. D.: 2015 SMOKE-Ready Canadian Air Pollutant Emission Inventory (APEI) Package, version 1, Zenodo [data set], <https://doi.org/10.5281/zenodo.4883639>, 2021.
- Seltzer, K. M., Pennington, E., Rao, V., Murphy, B. N., Strum, M., Isaacs, K. K., and Pye, H. O. T.: Reactive organic carbon emissions from volatile chemical products, *Atmos. Chem. Phys.*, 21, 5079–5100, <https://doi.org/10.5194/acp-21-5079-2021>, 2021.
- Sharma, A., Srivastava, S., Mitra, D., and Singh, R. P.: Spatiotemporal distribution of air pollutants during a heat wave-induced forest fire event in Uttarakhand, *Environ. Sci. Pollut. Res.*, 30, 110133–110160, <https://doi.org/10.1007/s11356-023-29906-7>, 2023.
- Sharma, A., Srivastava, S., Kumar, R., and Mitra, D.: Source attribution of carbon monoxide over Northern India during crop residue burning period over Punjab, *Environmental Pollution*, 359, 124707, <https://doi.org/10.1016/j.envpol.2024.124707>, 2024.
- Shephard, M. W., Dammers, E., Cady-Pereira, K. E., Kharol, S. K., Thompson, J., Gainariu-Matz, Y., Zhang, J., McLinden, C. A., Kovachik, A., Moran, M., Bittman, S., Sioris, C. E., Griffin, D., Alvarado, M. J., Lonsdale, C., Savic-Jovicic, V., and Zheng, Q.: Ammonia measurements from space with the Cross-track Infrared Sounder: characteristics and applications, *Atmos. Chem. Phys.*, 20, 2277–2302, <https://doi.org/10.5194/acp-20-2277-2020>, 2020.

- Shibata, Y. and Morikawa, T.: Review of the JCAP/JATOP Air Quality Model Study in Japan, *Atmosphere*, 12, 943, <https://www.mdpi.com/2073-4433/12/8/943> (last access: 27 October 2025), 2021.
- Smaran, M. and Voj, V.: Evaluation of Background Black Carbon Concentration in India, *Aerosol Air Qual. Res.*, 24, 230300, <https://doi.org/10.4209/aaqr.230300>, 2024.
- Smith, S. J., van Aardenne, J., Klimont, Z., Andres, R. J., Volke, A., and Delgado Arias, S.: Anthropogenic sulfur dioxide emissions: 1850–2005, *Atmos. Chem. Phys.*, 11, 1101–1116, <https://doi.org/10.5194/acp-11-1101-2011>, 2011.
- Smith, S. J., McDuffie, E. E., and Charles, M.: Opinion: Coordinated development of emission inventories for climate forcers and air pollutants, *Atmos. Chem. Phys.*, 22, 13201–13218, <https://doi.org/10.5194/acp-22-13201-2022>, 2022.
- Smith, T., Jalkanen, J.-P., Anderson, B. A., Corbett, J. J., Faber, J., Hanayama, S., O’Keeffe, E., Parker, S., Johanasson, L., Aldous, L., Raucchi, C., Traut, M., Ettinger, S., Nelissen, D., Lee, D. S., Ng, S. C., Agrawal, A., Winebrake, J. J., Hoen, M. T., Chesworth, S., and Pandey, A.: Third IMO GHG Study, MEPC-67-6-INF3-2014, <https://wwwcdn.imo.org/localresources/en/OurWork/Environment/Documents/ThirdGreenhouseGasStudy/GHG3ExecutiveSummaryandReport.pdf> (last access: 4 November 2025), 2015.
- Solazzo, E., Crippa, M., Guizzardi, D., Muntean, M., Choulga, M., and Janssens-Maenhout, G.: Uncertainties in the Emissions Database for Global Atmospheric Research (EDGAR) emission inventory of greenhouse gases, *Atmos. Chem. Phys.*, 21, 5655–5683, <https://doi.org/10.5194/acp-21-5655-2021>, 2021.
- Soulie, A., Granier, C., Darras, S., Zilbermann, N., Doumbia, T., Guevara, M., Jalkanen, J.-P., Keita, S., Lioussé, C., Crippa, M., Guizzardi, D., Hoesly, R., and Smith, S. J.: Global anthropogenic emissions (CAM5-GLOB-ANT) for the Copernicus Atmosphere Monitoring Service simulations of air quality forecasts and reanalyses, *Earth Syst. Sci. Data*, 16, 2261–2279, <https://doi.org/10.5194/essd-16-2261-2024>, 2024.
- Sun, W., Shao, M., Granier, C., Liu, Y., Ye, C. S., and Zheng, J. Y.: Long-Term Trends of Anthropogenic SO₂, NO_x, CO, and NMVOCs Emissions in China, *Earth’s Future*, 6, 1112–1133, <https://doi.org/10.1029/2018EF000822>, 2018.
- Thongsame, W., Henze, D. K., Kumar, R., Barth, M., and Pfister, G.: Evaluation of WRF-Chem PM_{2.5} simulations in Thailand with different anthropogenic and biomass-burning emissions, *Atmospheric Environment: X*, 23, 100282, <https://doi.org/10.1016/j.aeaoa.2024.100282>, 2024.
- Tong, D., Zhang, Q., Liu, F., Geng, G., Zheng, Y., Xue, T., Hong, C., Wu, R., Qin, Y., Zhao, H., Yan, L., and He, K.: Current Emissions and Future Mitigation Pathways of Coal-Fired Power Plants in China from 2010 to 2030, *Environmental Science & Technology*, 52, 12905–12914, <https://doi.org/10.1021/acs.est.8b02919>, 2018.
- Travis, K. R., Jacob, D. J., Fisher, J. A., Kim, P. S., Marais, E. A., Zhu, L., Yu, K., Miller, C. C., Yantosca, R. M., Sulprizio, M. P., Thompson, A. M., Wennberg, P. O., Crounse, J. D., St. Clair, J. M., Cohen, R. C., Laughner, J. L., Dibb, J. E., Hall, S. R., Ullmann, K., Wolfe, G. M., Pollack, I. B., Peischl, J., Neuman, J. A., and Zhou, X.: Why do models overestimate surface ozone in the Southeast United States?, *Atmos. Chem. Phys.*, 16, 13561–13577, <https://doi.org/10.5194/acp-16-13561-2016>, 2016.
- Twigg, M. V.: Catalytic control of emissions from cars, *Catalysis Today*, 163, 33–41, <https://doi.org/10.1016/j.cattod.2010.12.044>, 2011.
- U.S. Environmental Protection Agency: Overview of EPA’s Motor Vehicle Emission Simulator (MOVES3), EPA-420-R-21-004, <https://nepis.epa.gov/Exe/ZyPDF.cgi?Dockkey=P1011KV2.pdf> (last access: 21 December 2021), 2021a.
- U.S. Environmental Protection Agency: 2017 National Emissions Inventory (NEI) Technical Support Document, <https://www.epa.gov/air-emissions-inventories/2017-national-emissions-inventory-nei-data#doc> (last access: 21 December 2021), 2021b.
- UNC: Community Modeling and Analysis System CMAS, SMOKE v4.7 User’s Manual, <https://www.cmascenter.org/smoke/> (last access: 27 October 2025), 2019.
- UNECE: 1999 Protocol to Abate Acidification, Eutrophication and Ground-level Ozone to the Convention on Long-range Transboundary Air Pollution, as amended on 4 May 2012, https://www.unece.org/fileadmin/DAM/env/documents/2013/air/eb/ECE.EB.AIR.114_ENG.pdf (last access: 1 July 2021), 2012.
- UNECE: Annual Report: Connecting countries, recovering better, driving progress, improving lives, Information Service, United Nations Economic Commission for Europe, Palais des Nations, CH-1211 Geneva10, Switzerland, https://unece.org/sites/default/files/2022-04/UNECE%20Annual%20Report_2021_Web%20%281%29_0.pdf (last access: 27 October 2025), 2021.
- US EPA: AP-42: Compilation of Air Emissions Factors, <https://www.epa.gov/air-emissions-factors-and-quantification/ap-42-compilation-air-emissions-factors> (last access: 27 October 2025), 2009.
- US EPA: Final report SPECIATE version 4.5 database development documentation, Report EPA/600/R-16/294 (Abt Associates, 2016), SPECIATE 4.5: Speciation Database Development Documentation, 30 September, https://www.epa.gov/sites/default/files/2016-09/documents/speciate_4.5.pdf (last access: 27 October 2025), 2016.
- van der A, R. J., Ding, J., and Eskes, H.: Monitoring European anthropogenic NO_x emissions from space, *Atmos. Chem. Phys.*, 24, 7523–7534, <https://doi.org/10.5194/acp-24-7523-2024>, 2024.
- Wang, Y., Xiao, H.-W., Yin, M.-J., Sun, Q.-B., Fu, F., Tao, J.-H., and Xiao, H.-Y.: Stable carbon isotope reveals high impact of fishing ship activities on total carbon from PM_{2.5} in Qingdao, China, *Environmental Pollution*, 362, 124958, <https://doi.org/10.1016/j.envpol.2024.124958>, 2024.
- Whaley, C. H., Butler, T., Adame, J. A., Ambulkar, R., Arnold, S. R., Buchholz, R. R., Gaubert, B., Hamilton, D. S., Huang, M., Hung, H., Kaiser, J. W., Kaminski, J. W., Knote, C., Koren, G., Kouassi, J.-L., Lin, M., Liu, T., Ma, J., Manomaiphiboon, K., Bergas Masso, E., McCarty, J. L., Mertens, M., Parrington, M., Peiro, H., Saxena, P., Sonwani, S., Surapipith, V., Tan, D. Y. T., Tang, W., Tanpipat, V., Tsigaridis, K., Wiedinmyer, C., Wild, O., Xie, Y., and Zuidema, P.: HTAP3 Fires: towards a multi-model, multi-pollutant study of fire impacts, *Geosci. Model Dev.*, 18, 3265–3309, <https://doi.org/10.5194/gmd-18-3265-2025>, 2025.
- Xu, H., Zhang, W., Ren, Y., Zhang, Y., Li, J., Zheng, S., Dai, R., Hu, J., Cheng, H., Shen, G., Shen, H., Ma, J.,

- and Tao, S.: Role of primary drivers leading to emission reduction of major air pollutants and CO₂ from global power plants, *Environment International*, 190, 108936, <https://doi.org/10.1016/j.envint.2024.108936>, 2024.
- Yin, Y., Chevallier, F., Ciais, P., Broquet, G., Fortems-Cheiney, A., Pison, I., and Saunois, M.: Decadal trends in global CO emissions as seen by MOPITT, *Atmos. Chem. Phys.*, 15, 13433–13451, <https://doi.org/10.5194/acp-15-13433-2015>, 2015.
- Zhao, M., Dai, T., Goto, D., Wang, H., and Shi, G.: Assessing the assimilation of Himawari-8 observations on aerosol forecasts and radiative effects during pollution transport from South Asia to the Tibetan Plateau, *Atmos. Chem. Phys.*, 24, 235–258, <https://doi.org/10.5194/acp-24-235-2024>, 2024.
- Zheng, B., Huo, H., Zhang, Q., Yao, Z. L., Wang, X. T., Yang, X. F., Liu, H., and He, K. B.: High-resolution mapping of vehicle emissions in China in 2008, *Atmos. Chem. Phys.*, 14, 9787–9805, <https://doi.org/10.5194/acp-14-9787-2014>, 2014.
- Zheng, B., Tong, D., Li, M., Liu, F., Hong, C., Geng, G., Li, H., Li, X., Peng, L., Qi, J., Yan, L., Zhang, Y., Zhao, H., Zheng, Y., He, K., and Zhang, Q.: Trends in China's anthropogenic emissions since 2010 as the consequence of clean air actions, *Atmos. Chem. Phys.*, 18, 14095–14111, <https://doi.org/10.5194/acp-18-14095-2018>, 2018.